The Pennsylvania State University

The Graduate School

Department of Electrical Engineering

APPLICATIONS AND ANALYSIS OF RAMAN LIDAR TECHNIQUES FOR MEASUREMENTS OF OZONE AND WATER VAPOR IN THE TROPOSPHERE

A Thesis in

Electrical Engineering

by

Steven T. Esposito

Submitted in Partial Fulfillment
of the Requirements
for the Degree of

Master of Science

May 1999

_____

Steven T. Esposito

We approve the thesis of Steven T. Esposito.

Date of Signature

C. Russell Philbrick Professor of Electrical Engineering Thesis Advisor	
Charles Croskey Professor of Electrical Engineering	
John D. Mitchell Professor of Electrical Engineering Interim Head of the Department of Electrical Engineering	

ABSTRACT

The Lidar Atmospheric Profile Sensor (LAPS) instrument is capable of simultaneously measuring profiles of ozone, water vapor, temperature, and optical extinction. The measurements are range-resolved in 75 m increments and recorded in 1 minute time steps. The measured profiles are integrated, for user selected intervals, to calculate and display the real-time atmospheric profiles with their associated errors, $\pm 1\sigma$ standard deviation. Water vapor measurements are obtained by taking the ratio of the first Stokes Raman shifted radiation scattered by H_2O and N_2 molecules in the scattering volume. Profiles of ozone are obtained from a Differential Absorption Lidar (DIAL) analysis of the Raman shifted radiation scattered by N_2 and O_2 molecules from the transmitted 4^{th} harmonic of the Nd:YAG laser at 266 nm. The LAPS instrument uses the "solar blind" portion of the ultraviolet spectrum to obtain measurements during daytime periods when large background limits visible measurements.

The approach used for analysis of data measured by the LAPS instrument is described with special emphasis on the recent measurements of ozone. Errors with the profile measurements of ozone are evaluated. The Raman lidar technique is shown to provide a new and unique capability to measure the ozone in the troposphere. Comparisons between the lidar profiles and point sensors on aircraft are used to verify the result.

Table of Contents

List of Figures

List of Tables

Acknowledgements

I would like to thank my advisor, Dr. Philbrick, for guiding me through my research and academics. He has taught me the value of being an independent learner as well as a curious observer. I would also like to thank my committee member, Dr. Croskey, for supporting my effort and giving me valuable feedback.

Thanks are due to Dan Lysak, Tom Petach, Karoline Mulik, Anil Nanduri, Mike Zugger, Professor John Carroll from the University of California at Davis for the aircraft measurements which are used for comparisons in this thesis, and many other people without whose support I may not have achieved my goal.

I would also like to thank my parents. I would not have achieved all I have without their support and understanding.

Chapter 1

Introduction

On a hot summer day in an urban environment, ozone levels frequently exceed the one-hour 120 ppb concentration, which is the National Ambient Air Quality Standard (NAAQS) for ozone. Tropospheric ozone events are not limited to urban areas where pollutants are high. Pollutant species and the ozone itself can be generated and transported, advected with the wind, hundreds of miles from where they are formed. It is important to monitor and characterize how tropospheric ozone and the chemicals that form this toxic substance are transported. Monitoring of profiles of water vapor distribution can help with this. Water vapor measurements are useful because they help to describe the net convective mixing in the atmosphere. Water vapor thus provides an important clue to what is going on in terms of atmospheric dynamics.

The past twenty years have brought new and exciting techniques to the scientific community for profiling of atmospheric properties. Currently, the state-of-the-art technique, Light Detection and Ranging (LIDAR), is making advancements in the field of atmospheric remote sensing. A Raman lidar can be described as a radar at optical wavelengths. It uses a high power laser to transmit an intense optical pulse, and then measures the backscattered photons, which are shifted from the fundamental wavelengths of the laser by Raman scattering. These wavelength shifts are characteristic of the rotational and vibrational energy states of the specific molecules in the atmosphere.

Penn State University's Department of Electrical Engineering and the Applied Research Laboratory have developed the Lidar Atmospheric Profile Sensor (LAPS)

instrument as a prototype for the United States Navy. LAPS is a Raman lidar instrument that uses molecular scattering properties of the species in the lower atmosphere to simultaneously measure profiles of ozone, water vapor, temperature, and optical extinction due to aerosol/particle contributions. The profiles are obtained each minute, with a vertical resolution of 75 meters.

The purpose of this thesis is to describe the current status of the development of data analysis techniques used for monitoring ozone and water vapor in the troposphere. The techniques developed and used by the Penn State University lidar group to measure ozone and water vapor in the troposphere will be discussed. Data will be presented that will show tropospheric ozone being transported approximately 60 miles from the polluted urban environment of Los Angeles to the high desert in Hesperia, California.

Chapter 2

Origin and Distribution of Tropospheric Ozone, Fine Particles and Water Vapor

2.1 Ozone

Ozone has several extremely important roles in the Earth's atmosphere. First and most important, ozone absorbs virtually all solar ultraviolet radiation between 200 and 300 nm which would otherwise be transmitted to the Earth's surface. The major components of the atmosphere, especially O_2, filter out solar ultraviolet radiation with wavelengths < 230 nm. At a wavelength of 230 nm, approximately 1 part in 10^{16} of the intensity of the overhead sun is transmitted through the atmosphere. At wavelengths longer than 230 nm, the only species in the atmosphere capable of significantly attenuating the sun's radiation is ozone. Although ozone is not as abundant as O_2 in the atmosphere, it has strong absorption at the critical wavelengths (240 - 300 nm), referred to as the Hartley band. At a wavelength of 250 nm, stratospheric ozone will allow less than 1 part in 10^{30} of the solar radiation to penetrate to the ground [Wayne, 1991].

Ozone occurs naturally in the stratosphere, where it is both produced and destroyed, resulting in an equilibrium density profile. However, manmade chemicals have aided in the destruction process of stratospheric ozone. In 1985, a hole in the stratospheric ozone layer above Antarctica was reported. It is thought that since the atmospheric conditions above Antarctica are unique, the appearance of the hole does not necessarily mean that ozone is being globally depleted throughout the stratosphere. Since this event, scientists worked to characterize the chemistry and transport mechanisms that make the ozone hole appear and disappear with seasonal trends.

Tropospheric ozone is also created and destroyed in a photochemical cycle involving molecular oxygen and nitrogen oxides. Sunlight provides the necessary energy for this cycle and then controls the equilibrium distribution of ozone. The presence of both natural and manmade chemicals provides additional production pathways to generate excess ozone. Since tropospheric ozone is formed from a photochemical reaction, ozone will tend to reach its highest concentration levels during the summer months as the solar intensity reaches its maximum. Several scientists, including researchers at Penn State University, are performing studies to try to characterize the vertical and horizontal transport of ozone in the troposphere (from polluted areas to non-polluted areas).

2.1.1 Stratospheric Ozone

Stratospheric ozone protects the earth from harmful ultraviolet rays by absorbing almost all of these rays. It is in fact the absorption of this radiation by ozone which causes the temperature in the region to increase, producing the stratosphere. There are not many ozone molecules in the stratosphere, when compared to an abundant molecule such as oxygen. Although ozone is not abundant, it protects life on Earth because of the strong absorption characteristics at the harmful wavelengths between 230 and 290 nm. It is the only significant atmospheric molecule absorbing these wavelengths. A decrease in the density of ozone in the stratosphere would allow this ultraviolet radiation to reach the Earth's surface in harmful doses. Figure 2.1 shows a profile of ozone density as a function of height. It illustrates the increase of protective ozone in the stratosphere.

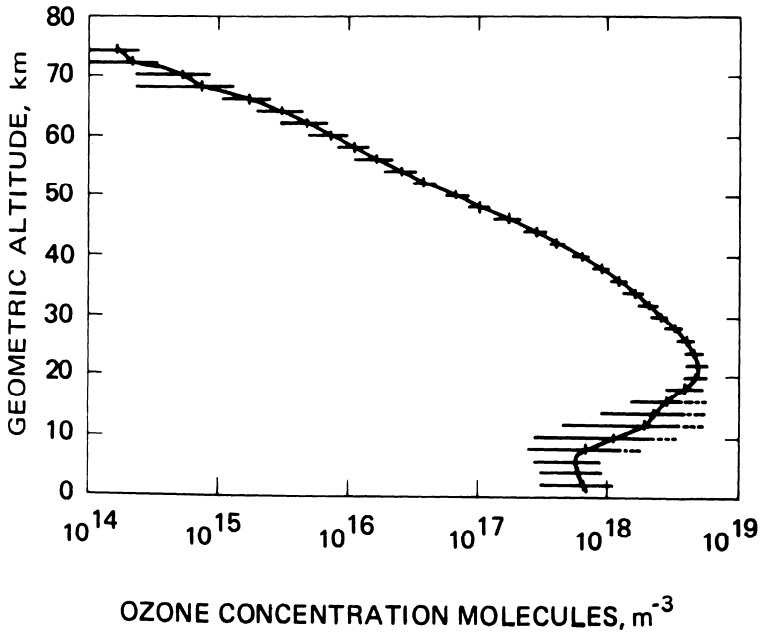

Figure 2.1. Mid-latitude ozone model density as a function of height [US Standard Atmosphere, 1976]. The horizontal bars indicate the typical range of ozone values expected at mid-latitudes.

In 1930, Sydney Chapman first proposed the theoretical explanation of the formation of ozone in the stratosphere. Five basic reactions that contribute to the formation of ozone were proposed. Ozone is formed from a three-body chemical process,

$$O + O_2 + M \rightarrow O_3 + M\,, \tag{2.1}$$

where M is any third atom or molecule. The atomic oxygen needed for this reaction is produced when the oxygen molecule is dissociated by solar radiation,

$$O_2 + h\nu(\lambda < 242.3\,\text{nm}) \rightarrow O + O\,. \tag{2.2}$$

Ozone is destroyed by photodissociation and by reaction with oxygen atoms.

$$O_3 + h\nu(\lambda < 1100\,\text{nm}) \rightarrow O + O_2 \quad (2.3)$$

$$O_3 + O \rightarrow 2O_2 \quad (2.4)$$

The atomic oxygen may undergo a three-body collision before forming ozone resulting in,

$$O + O + M \rightarrow O_2 + M \quad (2.5)$$

[Liou, 1980]. These five reactions describe the chemical reactions that control ozone concentration in the stratosphere. These reactions occur simultaneously, creating and destroying ozone in the stratosphere to produce an equilibrium profile. The only way the overall ozone concentration in the stratosphere is changed is by introducing manmade chemicals that change the production and loss processes.

Scientific study has shown that chlorofluorocarbons (CFCs) are one of the main reasons for stratospheric ozone depletion. CFCs are used in products such as refrigerators, air conditioners, cleaning solvents, fire extinguishers, and aerosol sprays, as well as in the manufacturing of disposable foam containers and insulators so often used by manufacturers. CFCs have a chemical lifetime in the atmosphere as long as 75 to 100 years. CFCs released into the lower atmosphere will eventually diffuse into the upper atmosphere where they can decompose and provide chlorine, fluorine and other chemicals which are not readily removed from the lower atmosphere by chemical decay or weather.

One CFC molecule can break down as many as 100,000 molecules of ozone. When CFCs reach the stratosphere, a chlorine containing molecule is dissociated by ultraviolet radiation. The chlorine atom is highly reactive and easily breaks a weak bond in an ozone molecule,

$$Cl + O_3 \rightarrow ClO + O_2 . \qquad (2.6)$$

The chlorine monoxide molecule can then react with an oxygen atom to free the chlorine,

$$ClO + O \rightarrow Cl + O_2 . \qquad (2.7)$$

This chlorine atom is then free to again break down an ozone molecule as in reaction 2.6. The chlorine molecule destroys many ozone molecules before it is eventually lost.

The depletion of the stratospheric ozone layer will continue to affect humans as well as plant life on earth. Excessive ultraviolet radiation can produce sunburn, skin cancer, cataracts, and impaired immune systems. Atmospheric weather patterns may also change as a result of this ozone depletion. The extreme seasonal variations in the formation of the ozone hole over the Antarctic region are due to storage of the active chemicals during the dark winter and the sudden release and activation of chemical reactions as the solar radiation returns in the spring.

2.1.2 Tropospheric Ozone

Ozone in the lower atmosphere is a major component of photochemical smog in urban environments and is harmful to human, plant, and animal health. A portion of

tropospheric ozone is transported downward by diffusion from the stratosphere. Tropospheric ozone is primarily produced in the first 50 meters of the surface layer from chemical reactions with oxides of nitrogen (NO_x) and volatile organic compound (VOC) molecules, in the presence of sunlight. VOCs escape as vapors from chemical plants, refineries, gas stations and motor vehicles. In addition to these sources, there is a natural source of biogenic VOCs from the oils in plant leaves, which are evaporated during periods of stress, particularly on hot summer days. Nitrogen oxides (NO_x) are emitted mostly from the combustion of fossil fuels, such as oil, gas, and coal [EPRI, 1988]. Strong sunlight causes ground level ozone to form in harmful concentrations. In the atmosphere, ozone is chemically produced by photolysis of NO_2 freeing an oxygen atom. This oxygen atom is then free to combine with an oxygen molecule to form ozone resulting in NO and O_3,

$$NO_2 + h\nu(\lambda < 380\,\text{nm}) \rightarrow NO + O \ , \tag{2.8}$$

$$O + O_2 + M = O_3 + M \ . \tag{2.9}$$

The product of this reaction usually reacts with one another to regenerate NO_2,

$$NO + O_3 \rightarrow NO_2 + O_2 . \tag{2.10}$$

These reactions tend to balance each other, resulting in no accumulation of ozone. However, if the NO produced in (2.8) is followed by reaction with HO_2 or other organic peroxy radicals (VOC'S), the NO will not be able to destroy the ozone molecule,

$$NO + HO_2 \rightarrow NO_2 + HO . \tag{2.11}$$

In this case, ozone is not destroyed in the regeneration of NO_2, resulting in the net production of ozone. Since the primary emission of concern from internal combustion engines is NO, it is easy to see that excess NO_2 and thus excess O_3 will be generated. The HO product produced in this reaction can then react with CO, methane and other organic molecules to regenerate HO_2, i.e.,

$$CO + HO \xrightarrow{O_2} CO_2 + HO_2 . \tag{2.12}$$

This contributes to the net production of ozone [Walceck and Yuan, 1994].

One of the most important photolysis reactions influencing net ozone formation, is the photolysis of ozone itself and the photolysis of formaldehyde (HCHO),

$$O_3 + h\nu \rightarrow O_2 + O(^1D) \tag{2.13}$$

$$HCHO + h\nu \xrightarrow{O_2} 2HO_2 + CO . \tag{2.14}$$

Although the reaction present in (2.13) slowly destroys ozone, it is also the dominant source of highly reactive free radicals. Reaction (2.14) is important if there are high concentrations of organic compounds (VOC'S). The HO_2 and CO radicals produced aid in the net formation of ozone by reacting with NO and HO, respectively [Walceck and Yuan, 1994].

Water vapor also plays an important role in regulating concentrations of short-lived and highly reactive HO_x radicals in the troposphere. Water combines with the highly reactive radical $O(^1D)$,

$$H_2O + O(^1D) \rightarrow 2HO. \quad (2.15)$$

The product of this reaction is the primary source of HO_x in the lower atmosphere. HO_x rapidly combines with CO and other organic constituents in the atmosphere. This reduces the number of organic compounds and HO_2, which are necessary for the formation of ozone [Walcek, 1994].

Water vapor also aids in the removal of free radicals from the atmosphere, especially under conditions of low NO_X concentration. Water reacts with the reactive radical HO_x,

$$H_2O + 2HO_2 \rightarrow H_2O_2 + O_2 + H_2O. \quad (2.16)$$

This reaction scavenges reactive HO_x, converting it to less reactive hydrogen peroxide (H_2O_2) [Walcek and Yuan, 1994].

Repeated exposure to ozone pollution can permanently damage the lungs of a human. Even a healthy person can experience difficulty in breathing whether they are participating in strenuous activity or rest activity. Since the formation of ozone at ground level is triggered when the solar radiation flux is highest, anyone spending time outdoors during the summer months can be affected, particularly children, the elderly, outdoor workers and people exercising. Ozone that is present in small amounts can trigger a variety of health problems such as chest pains, coughing, nausea, throat irritation, and congestion. It will also aggravate individuals with preexisting conditions such as bronchitis, heart disease, emphysema, and asthma [EPA, 1997].

During summer months, tropospheric ozone frequently reaches and exceeds the one-hour 120 ppb National Ambient Air Quality Standard (NAAQS) in high pollution regions. A new standard of 80 ppb for 8 hours is currently being adopted, instead of the 120 ppb peak value. Tropospheric ozone has a typical lifetime of two to three days before it is destroyed between the surface and 30 meters height as it contacts surfaces and oxidizes them (leaves, earth etc.). The major contributing factors to the formation of ozone are the pollutants put into the atmosphere by human activities. Tropospheric ozone is not limited to areas where these pollutants are high. A significant fraction of the ozone produced on hot summer days is associated with biogenic VOCs from trees. Pollutant gases, including ozone itself, can be generated and transported with wind hundreds of miles. Scientists are currently trying to characterize the vertical and horizontal transport mechanisms that contribute to the formation and transportation of tropospheric ozone. Since the density of pollutants in the atmosphere changes constantly with time, the monitoring of tropospheric ozone can only be accomplished with frequent and precise measurements at many altitudes. Measurements must be frequent enough to distinguish between the short term variations of tropospheric ozone due to pollution sources and the seasonal and annual cycles. Penn State University's Department of Electrical Engineering and the Applied Research Laboratory have developed an instrument capable of measuring ozone profiles, in ppb, from the surface to 3 km above the surface of the earth. The instrument is the LAPS (Lidar Atmospheric Profiler Sensor) lidar (Light Detection and Ranging) instrument. This instrument provides both the height and time resolution needed to describe the distribution of ozone in real time. This

instrument is a Raman lidar that uses a DIAL technique to obtain profiles of ozone in the troposphere. The technique is described in Chapter 3.

2.2 Fine Particles

Fine particles are generally measured using standardized filter technology to determine densities of particulate matter (PM). $PM_{2.5}$ and PM_{10} refer to standard techniques developed to measure particles with aerodynamic diameters less than 2.5 and 10 μm, respectively. PM is not the measure of any particular particle or compound, but the integrated mass of airborne particles that are suspended in complex mixtures of aerosol particles including particles produced from photochemical reactions of VOCs and NO_X [Hidy et al., 1998]. Sources, size, chemical composition, and atmospheric behavior divide particles into "fine and coarse modes", these modes are divided at about 2.5 μm for monitoring purposes.

Coarse particles (aerodynamic diameters 2.5 - 10 μm) are generated primarily by mechanical processes that break down the Earth's surface materials into dust that can be suspended by the wind, agricultural practices, and vehicular traffic. Industrial processes also contribute to ambient levels of coarse particles in some areas. Coarse-mode particles are efficiently removed by gravitational settling and have atmospheric lifetimes ranging from minutes to hours. Fine particles (aerodynamic diameters ≤ 2.5 μm) result primarily from the combustion of fossil fuels and industrial boilers, automobiles, power generation plants, and residential heating systems. A significant portion of fine particles in the atmosphere is produced through the chemical conversion of anthropogenic and natural

precursor emissions (SO_2, NO_X, reactive organics, etc.). Fine particles can remain suspended for periods of time ranging from days to weeks, and contribute to ambient PM levels hundreds of miles away from where they are formed [PM Measurement Workshop, 1998]. Frequently, good correlation occurs between the density of fine particles in the atmosphere and the formation of tropospheric ozone.

The regional background of fine particles is typically highest in the eastern United States in the summer months, while levels typically peak in winter months in southern California. The average visual range in most of the western United States is 60-90 miles, which is one-half to two-thirds of what it would be without air pollution. The average visual range in the eastern United States is less than 18 miles, or about one-fifth of the visual range that would exist without air pollution [PM Measurement Workshop, 1998].

Studies have concluded that tropospheric aerosols have been associated with adverse health impacts. Fine and coarse particles both find their way into the human respiratory tract. The path these particles use to enter, as well as the density of the particles deposited, depends on the individual (mouth versus nose breathing) and the particle characteristics. The deposition of inhaled particles in different regions of the respiratory tract is shown as a function of particle size in Figure 2.2 [PM Measurement Workshop, 1998]. Figure 2.2 illustrates that $PM_{2.5}$ particles are of most concern to human health. In fact, it has been suggested that $PM_{2.5}$, the sum of particles smaller than 2.5 μm, should be used as a measure of the exposure and dosage due to tropospheric aerosols [Hidy, 1998].

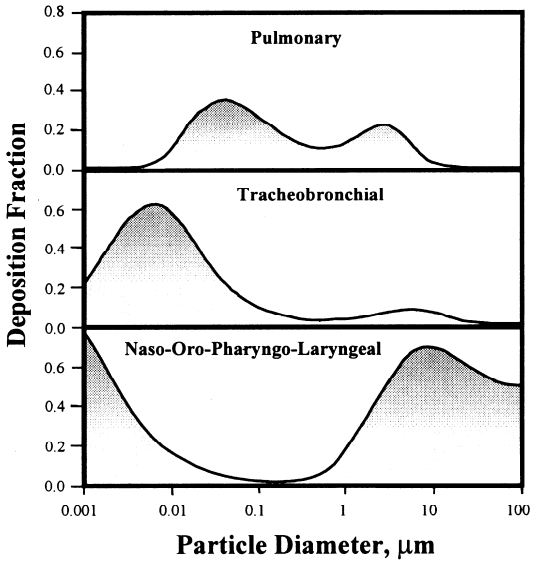

Figure 2.2. Fractional deposition in various regions of the respiratory system as a function of particle size for an average adult male.

Studies show that tropospheric aerosols increase mortality, hospital admissions and respiratory symptoms, and that pulmonary-function decreases with increasing ambient particle mass concentrations [Hidy, 1998]. It is important to monitor and characterize conditions where these aerosols form and transport mechanisms that distribute these aerosols. The Penn State University's Electrical Engineering Department and Applied Research Laboratory lidar group have developed techniques using lidar measurements to estimate the density of aerosols in the troposphere. The process uses the lidar return signal to obtain extinction profiles at specific wavelengths. Since the extinction due to the molecular component is well known in the troposphere, any deviation of the return signal from the expected molecular extinction profile is due to aerosol extinction. This provides information on the aerosol density present in the troposphere.

2.3 Water Vapor

The largest concentration of atmospheric water vapor is found in the lower troposphere. Water vapor, like carbon dioxide and ozone, is a greenhouse gas. When an object is warmed by radiation, it re-radiates that energy at longer wavelengths. The earth is warmed primarily by the visible wavelengths and is cooled by surface radiation at the longer infrared wavelengths. Water vapor, carbon dioxide and ozone in the atmosphere absorb the infrared energy emitted from the earth. Figure 2.3 illustrates the absorption of infrared energy by water vapor, carbon dioxide and ozone. Trapping of thermal infrared radiation by atmospheric gases is typical of the atmosphere and is referred to as the greenhouse effect [Liou, 1980]. If it were not for this natural greenhouse effect, the Earth's surface would be approximately 33 °C (60 °F) colder than it is today. Under clear sky conditions, roughly 60-70 % of the natural greenhouse effect is due to water vapor, which is the dominant greenhouse gas in Earth's atmosphere [Schloerer, 1997].

Water vapor transfers energy from the tropics and regulates the Earth’s temperature across the surface of the earth. When water vapor evaporates, latent heat is transferred into the atmosphere and when is condenses, sensible heat is extracted by the atmosphere [Peixoto, 1992]. A process known as the hydrological cycle describes the water vapor cycle in the atmosphere. Evaporation of water from the oceans and continents or transpiration of water by plants and animals into the atmosphere under the direct or indirect influence of solar energy occurs in this process. In the atmosphere, water is transported in the condensed phase as clouds, or in the vapor phase as water vapor. It then falls on the continents and oceans in the form of rain, snow, hail or other forms of precipitation. The water then returns to the atmosphere through evaporation

from surface water and soil or transpiration from plants and animals, thus completing the cycle. A diagram of the hydrological cycle can be seen in Figure 2.4 [Peixoto, 1992].

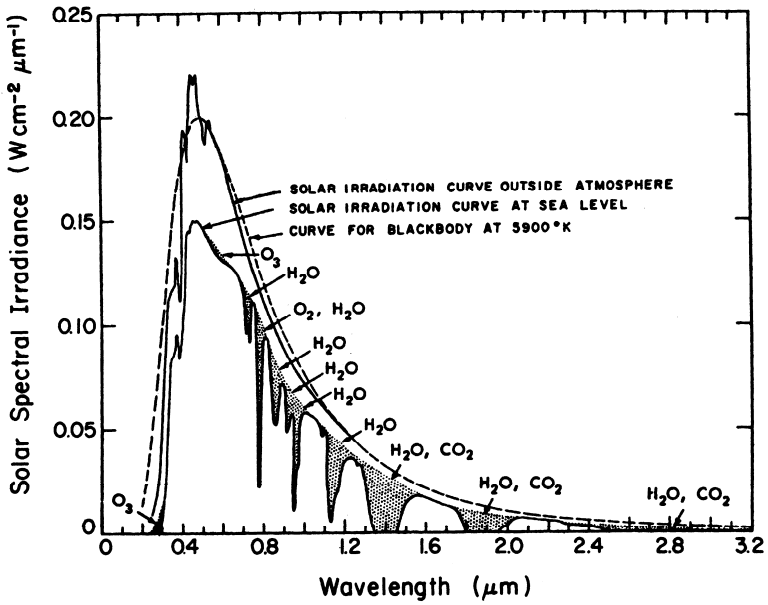

Figure 2.3. Spectral irradiance of direct sunlight before and after it passes through the earth's atmosphere. The stippled portion show the atmospheric absorption of various molecules [Measures, 1984].

From this cycle, it is evident that the monitoring of water vapor is useful in a polluted atmosphere because it helps to determine the net convective mixing in the atmosphere. The local profile of water vapor provides a tracer for convective mixing and horizontal transport to help describe the atmospheric dynamics.

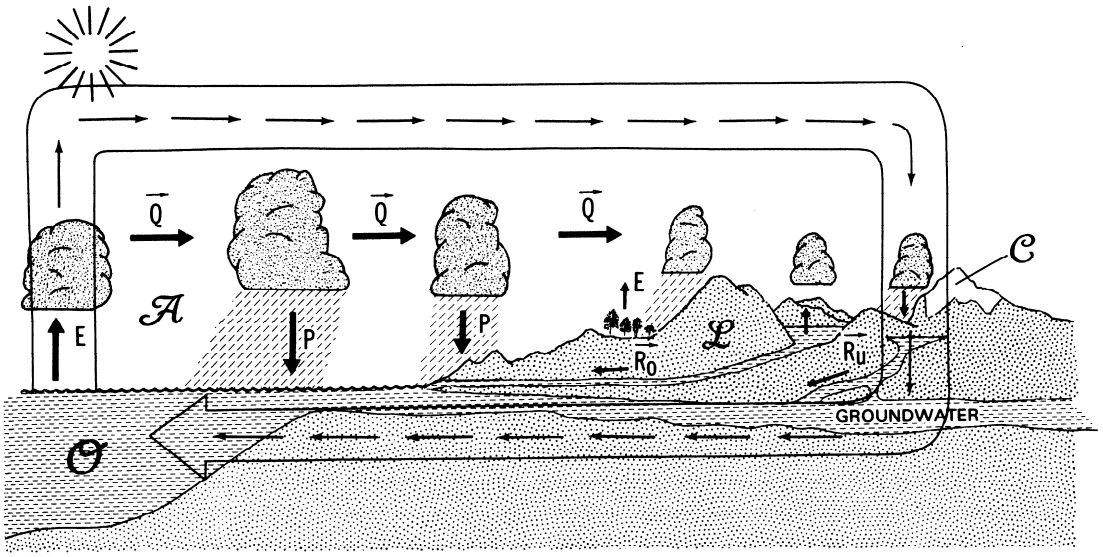

Figure 2.4. Schematic diagram of the atmospheric and terrestrial branches of the hydrological cycle showing the importance of evaporation E, advection of water vapor in the atmosphere Q, precipitation P, river runoff R_0, and underground runoff R_U [Peixoto, 1992].

Thus, monitoring water vapor can help characterize the vertical and horizontal transport of fine particles in the atmosphere. This is important when trying to predict when surface pollution events may or may not occur. As previously mentioned, water vapor also plays an important role in reacting with HO_x, converting it to less reactive hydrogen peroxide (H_2O_2).

It has been shown that the monitoring of water vapor can give a great deal of useful information, in particular, it provides a continuous monitor of the height and convective activity of the planetary boundary layer. At high relative humidity (RH), the water vapor is responsible for the rapid growth of the sulfate aerosols, which dominate the eastern aerosol population type. The water vapor can add factors of 3 to 5 to the

sulfate aerosol as the RH increases from 70 to 95%. The lidar group at Penn State University has developed Raman lidar techniques to continuously monitor water vapor. This technique can produce measurements of water vapor from the surface to 3 km during the day, and from the surface to 5 km during the night.

Chapter 3

Lidar Techniques for Measurements of Water Vapor and Ozone

3.1 Introduction to Lidar

In the near future, the routine monitoring of atmospheric and meteorological properties will be accomplished using a lidar (Light Detection and Ranging) instrument. Lidar is a radar at optical wavelengths with a laser transmitter and a light collection receiver consisting of a telescope and detection electronics. The laser transmitter sends a pulsed beam to scatter from the molecules and particles in the atmosphere. The measurement is range-resolved since the arrival time of the backscattered light pulse provides a precise altitude for the scattering volume [Philbrick and Lysak, 1998]. The intensity of the backscattered light at the transmitted wavelength, as well as several frequency shifted wavelengths, is directly proportional to atmospheric properties such as water vapor, ozone, temperature, and optical extinction. Two of these lidar instruments, LAMP (Laser Atmospheric Measurements Profiler) [Stevens, 1992] and LAPS (Lidar Atmospheric Profiler Sensor) [Philbrick et al., 1997], have been developed at Penn State University by the Department of Electrical Engineering and the Applied Research Laboratory.

3.2 The LAPS lidar instrument

The LAPS lidar instrument was developed at Penn State as a prototype instrument to predict RF refraction for the United States Navy, and fabrication of the prototype was completed in 1996. This instrument was designed with improvements based upon the

results of tests and lessons learned from five previous lidar research instruments. The LAPS lidar is a rugged instrument, with fully automated operation, which makes it deployable in virtually any environment. The LAPS lidar has been designed with more than twenty sub-systems to control and simplify its operation. The primary subsystems of the LAPS lidar instrument can be seen in Table 3.1.

Table 3.1 Primary sub-system of LAPS lidar instrument.

Transmitter	Continuum 9030 – 30 Hz 5X Beam Expanded	600 mj at 532 nm 130 mj at 266 nm
Receiver	61 cm diameter	Fiber optic transfer
Detector	Seven PMT channels	528 and 530 nm – Temperature 660 and 607 nm - Water Vapor 295 and 284 nm - Daytime Water Vapor 277 and 284 nm - Raman/DIAL Ozone
Data System	DSP 100 MHZ count rate	75 meter range bins
Safety Radar	Marine R-70 X-Band	Protects 6° cone angle around beam

The LAPS instrument is contained in two separate units. The first is a weather-sealed container housing the transmitter and receiver. This sealed unit has been designed to include environmental control, calibration, performance self-tests, and built-in-tests to check many functions [Philbrick et al., 1997]. The transmitter is a high power Nd:YAG laser with a primary wavelength at 1064 nm. Nonlinear crystals are used to double and quadruple the primary frequency to produce output wavelengths at 532 and 266 nm. The laser operates at a pulse repetition rate of 30 Hz, emitting 8 ns pulses with energies of 600 mj and 130 mj at the respective wavelengths. Two hard-coated mirrors are used to steer

the beam of laser pulses into the atmosphere through a weather-sealed window. The LAPS receiver is arranged as a prime focus paraboloid telescope, which focuses the backscattered light onto a one millimeter optical fiber which transfers the signal to the detector system. A diagram of the LAPS transmitter and receiver configuration can be seen in Figure 3.1.

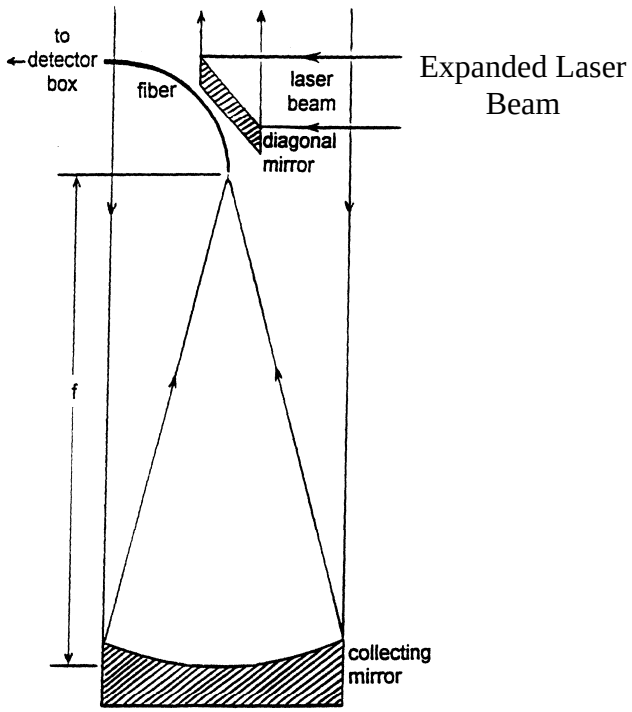

Figure 3.1. LAPS transmitter and receiver [Jenesse et al, 1997].

The second unit of the LAPS instrument system consists of a control console that houses the detector box, the data collection electronics, and two computers. One

computer controls and monitors the laser and detection electronics and processes the one minute raw data files, while the other displays the real time atmospheric data.

The detector box for the LAPS lidar instrument was designed for low altitude measurement using Raman vibrational and rotational scattering techniques. The Raman shifted signals derived from the transmitted 532 nm and 266 nm wavelengths are split with beam splitters and focused into photomultiplier tubes. A diagram of the LAPS detector box can be seen in Figure 3.2.

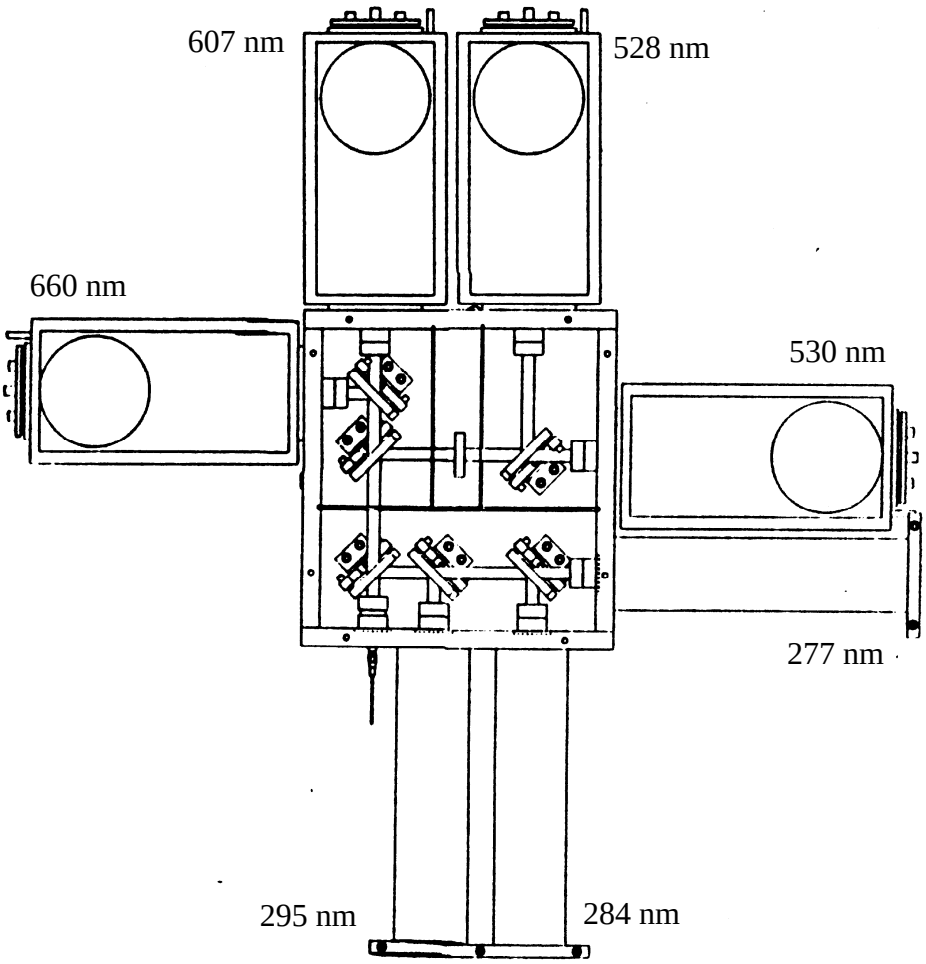

Figure 3.2. LAPS detector box layout.

Photon counting techniques are used to measure the amount of backscatter received from the molecules in the atmosphere. The data collection unit for each channel consists of a photomultiplier tube, amplifier, discriminator, counter, and accumulator. The return signal is integrated for one minute in 75 meter range bins and then transferred to a computer.

3.3 Raman Scattering

Raman (inelastic) scattering cross sections for vibrational Stokes scattering from atmospheric molecules are about three orders of magnitude smaller than the corresponding Rayleigh scattering cross sections. The scattered signal consists of radiation that has suffered a frequency shift that is characteristic of the stationary energy states of the irradiated molecule [Measures, 1992]. When incident photons collide with a molecule, an instantaneous virtual energy is associated with the molecules. In most cases, the molecule returns to ground state and the photon is scattered with an energy similar to the initial photon, only shifted slightly by the Doppler velocity of the molecule. However in some cases, energy is given up to the molecule resulting in the scattered photons having lower energy. These scattered photons have lower frequency, longer wavelength, Stokes radiation. The frequency shifts are limited to the energy quanta associated with the vibrational energy states of the particular molecule. If the molecule is already in an excited state, the incident photons may gain energy from the molecule by returning to the ground state. The scattered photons will also have increased energy, higher frequency, shorter wavelength, which is referred to as anti-Stokes radiation. Figure 3.3 illustrates the Stokes and anti-Stokes scattering processes. The right side of

the figure shows the first Stokes vibrational shifts for O_2 and H_2O with their associated rotational Raman shifts, when excited by a laser at 532 nm. The elastic signal, at 532 nm, is also shown with its associated rotational Raman shifts.

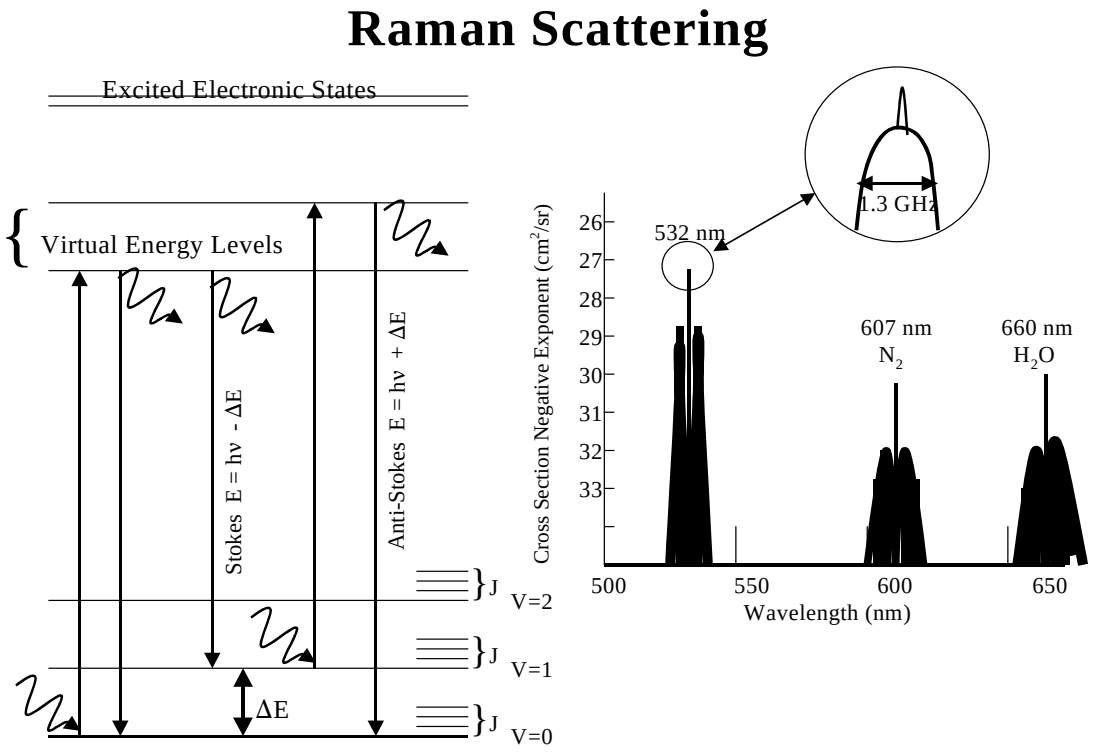

Figure 3.3. Representation of Raman vibrational Stokes and anti-Stokes scattering. The rotational and vibrational first Stokes wavelength shifts are shown for 532 nm transmission of a Nd:YAG laser.

3.4 Raman Lidar Measurement Techniques

The LAPS lidar instrument uses the Raman scattering technique to retrieve measurements proportional to ozone density, nitrogen density, oxygen density, water vapor concentration and temperature. The real time data processing of the LAPS instrument takes ratios of the Raman shifted return signals to obtain profiles of water

vapor, ozone, temperature, and optical extinction. This has the major advantage of essentially removing all uncertainties within the lidar equation. These uncertainties include telescope form factor, requirement for knowledge of the absolute detector sensitivity, and non-linear factors caused by aerosol and cloud scattering.

A summary of the LAPS lidar measurement capabilities can be seen in Table 3.2. The LAPS lidar collects the rotational Raman backscatter at 528 nm and 530 nm and the vibrational Raman backscatter at 607 nm, 660 nm, 277 nm, 284 nm and 295 nm. The 607 and 660 nm signals are the 1st Stokes vibrational Raman shifts from the N_2 and H_2O molecules in the atmosphere excited by the second harmonic of the Nd:YAG laser (532 nm). The 277, 284 and 295 nm signals are the 1st Stokes vibrational Raman shifts from the O_2, N_2, and H_2O molecules in the atmosphere excited by the fourth harmonic of the Nd:YAG laser (266 nm). A measurement sensitive to atmospheric temperature is obtained by taking the ratio of the rotational Raman backscatter at 528 and 530 nm. A measurement sensitive to water vapor concentration can be obtained by taking the ratio of 660nm/607nm and 295nm/284nm. The ratio of 295nm/284nm must be corrected for tropospheric ozone absorption. A measurement sensitive to tropospheric ozone can be found by taking the ratio of 277nm/284nm. This ozone measurement is then applied to the 295nm/284nm ratio to correct the daytime water vapor and is used by itself as a measure of tropospheric ozone.

Table 3.2 LAPS measurement capabilities using Raman scattering techniques.

Property	Measurement	Altitude (km)	Time Resolution
Water Vapor	660/607 Raman 295/284 Raman	Surface to 5 Surface to 3	Night - 1 min. Day/Night - 1 min.
Temperature	528/530 Rotational Raman	Surface to 5	Night - 30 min.
Optical Extinction - 530 nm	530 nm Rotational Raman	Surface to 5	Night 10 to 30 min.
Optical Extinction - 607 nm	607 nm Vibrational Raman	Surface to 5	Night 10 to 30 min.
Optical Extinction - 284 nm	284 nm Vibrational Raman	Surface to 3	Day/Night 30 min.
Ozone	277/285 Raman/DIAL	Surface to 2 - 3	Day/Night 30 min.

3.5 LAPS Measurement of Water Vapor

Water vapor content can be expressed by taking the ratio of its number density to the number density of ambient air. Nitrogen is used to determine the density of ambient air since it represents a constant, well-known portion of dry air in the atmosphere. This ratio is known as the water vapor mixing ratio, or specific humidity, and is usually given in units of grams per kilogram [Harris, 1996]. The water vapor mixing ratio can be obtained from the following relation,

$$W(z) = K * \frac{S_{H2O}(Z)}{S_{N2}(Z)} \qquad (3.1)$$

.

where,

S_{H2O} is the received signal from the Raman shift of H_2O,
S_{N2} is the received signal from the Raman shift of N_2,
K is a calibration constant.

K is determined by fitting the ratio of the two lidar signals of H_2O and N_2 with the simultaneous average of water vapor data from radiosonde balloons. Many of the unknown factors in the lidar equation are cancelled out by taking the ratio of the return signals; however, molecular scattering and ozone absorption (at ultraviolet wavelengths) are wavelength dependent parameters that do not cancel out in this ratio. The dependence can be illustrated by taking the ratio of the signals in the lidar equation.

The power of a signal measured by a monostatic lidar at a given wavelength is,

$$P(\lambda_R, z) = E_T(\lambda_T)\xi_T(\lambda_T)\xi_R(\lambda_R)\frac{c\tau}{2}\frac{A}{z^2}\beta(\lambda_T, \lambda_R)\exp\left[-\int_0^z [\alpha(\lambda_T, z') + \alpha(\lambda_R, z')]dz'\right] \qquad (3.2)$$

where,

z is the altitude of the volume element where the return signal is scattered,
λ_T is the wavelength of the laser light transmitted,
λ_R is the wavelength of the laser light received,
$E_T(\lambda_T)$ is the light energy per laser pulse transmitted at wavelength λ_T,
$\xi_T(\lambda_T)$ is the net optical efficiency at wavelength λ_T of all transmitting devices,
$\xi_R(\lambda_R)$ is the net optical efficiency at wavelength λ_R of all receiving devices,
c is the speed of light,
τ is the time duration of the laser pulse,
A is the area of the receiving telescope,
$\beta(\lambda_T,\lambda_R)$ is the back scattering cross section of the volume scattering element for the laser wavelength λ_T at Raman shifted wavelength λ_R,
$\alpha(\lambda,z')$ is the extinction coefficient at wavelength λ at range z'.

The extinction coefficient is equal to the sum of the absorption by chemical species and the scattering by molecules and particles in the atmosphere.

$$\frac{P_{H20}(z)}{P_{N2}(z)} = \frac{\xi_R(\lambda_{H2O})}{\xi_R(\lambda_{N2})} \frac{\beta(\lambda_T, \lambda_{H2O}, z)}{\beta(\lambda_T, \lambda_{N2}, z)} \frac{\exp\left[-\int_0^z [\alpha(\lambda_{H2O}, z')]dz'\right]}{\exp\left[-\int_0^z [\alpha(\lambda_{N2}, z')]dz'\right]} \tag{3.3}$$

A constant is introduced to simplify the calculation,

$$k_{systen} = \frac{\xi_R(\lambda_{H2O})}{\xi_R(\lambda_{N2})} \frac{\beta(\lambda_T, \lambda_{H2O}, z)}{\beta(\lambda_T, \lambda_{N2}, z)} = \frac{\xi_R(\lambda_{H2O})}{\xi_R(\lambda_{N2})} \frac{\sigma_{H2O}}{\sigma_{N2}} \frac{N_{H2O}}{N_{N2}} \tag{3.4}$$

where,

σ_{H2O} is the Raman cross-section of water at the laser wavelength,
σ_{N2} is the Raman cross-section of nitrogen at the laser wavelength,
N_{H2O} is the concentration of water in the atmosphere,
N_{N2} is the concentration of nitrogen in the atmosphere.

This constant was determined experimentally for the LAPS instrument by the comparison of simultaneous profiles from meteorological balloons and lidar measurements.

The extinction coefficient is assumed to equal the sum of the scattering due to molecules, the scattering due to aerosols along the path, and the absorption of ozone. The ratio becomes,

$$\frac{P_{H20}(z)}{P_{N2}(z)} = k_{system} \frac{\exp\left[-\int_0^z [\alpha_m(\lambda_{H2O}, z') + \alpha_a(\lambda_{H2O}, z') + \alpha_{O3}(\lambda_{H2O}, z')]dz'\right]}{\exp\left[-\int_0^z [\alpha_m(\lambda_{N2}, z') + \alpha_a(\lambda_{N2}, z') + \alpha_{O3}(\lambda_{N2}, z')]dz'\right]} \quad (3.5)$$

where,

$\alpha_m(\lambda_x,z)$ is the attenuation due to molecular scattering at wavelength λ_x,
$\alpha_a(\lambda_x,z)$ is the attenuation due to absorption and scattering of aerosols at wavelength λ_x,
$\alpha_{O3}(\lambda_x,z)$ is the attenuation due to ozone absorption at wavelength λ_x.

The relative difference between the absorption and scattering due to aerosols at the two wavelengths is small and is neglected, so equation 3.5 is simplified to:

$$\frac{P_{H20}(z)}{P_{N2}(z)} = k_{system} * \exp\left[-\int_0^z [\alpha_m(\lambda_{H2O}, z') - \alpha_m(\lambda_{N2}, z') + \alpha_{O3}(\lambda_{H2O}, z') - \alpha_{O3}(\lambda_{N2}, z')]dz'\right] \quad (3.6)$$

3.5.1 Molecular Scattering Correction for Water Vapor

In order to derive an accurate water vapor measurement from the ratio of H_2O/N_2, the ratio must be corrected for the molecular scattering at the Raman shifted wavelengths. The molecular scattering in this equation is calculated using the standard profile (height dependence) of the atmosphere since pressure, temperature, and humidity are known at ground level. The molecular scattering at each wavelength can be represented as,

$$\sigma_x K(z) = \int_0^z \alpha_m(\lambda_x, z')dz' = \sigma_x \int_0^z \left[NH\left(1 - \exp\left(\frac{-z'}{H}\right)\right)dz' \right] \tag{3.7}$$

$$H = \frac{kT(z)}{mg} \tag{3.8}$$

$$T(z) = To + \gamma\, z \tag{3.9}$$

where,

N is the number density at ground level,
k is Boltzman's constant (1.380658 x 10^{-34}),
m is average mass per molecule,
g is gravitational acceleration,
To is the surface temperature,
γ is the lapse rate of -6.5 K/km (valid only for the lower 10 km),
σ_x is the Rayleigh scattering cross-section at the x^{th} Raman shifted wavelength.

The molecular component of the signal loss can thus be removed from the data based upon the molecular scattering cross sections and the fractional abundance of N_2 and O_2.

The water vapor mixing ratio calculated from the 1st Stokes vibrational Raman shift from the 2nd harmonic of the Nd:YAG laser (532 nm) does not need to be corrected for ozone absorption. The absorption due to ozone is zero in this case, i.e. $\alpha_{O3}(\lambda_x, z) = 0$. The measurement for this case only needs to be corrected for molecular scattering. The corrected expression is,

$$W(z) = K * \frac{S_{H2O}(Z)}{S_{N2}(Z)} \exp(\sigma_{H2O} - \sigma_{N2})K(z) \tag{3.10}$$

Thus, the specific humidity is primarily proportional to the ratio of two Raman signals. The difference in the aerosol extinction at the two wavelengths depends upon the amount of aerosol present and the weak wavelength dependence between these two scattered wavelengths. Figure 3.4 illustrates the weak wavelength dependence of aerosols in low and high-altitude cloud haze. The wavelength dependence of the aerosol extinction coefficient between 660 and 607 nm or between 295 and 284 nm is very weak.

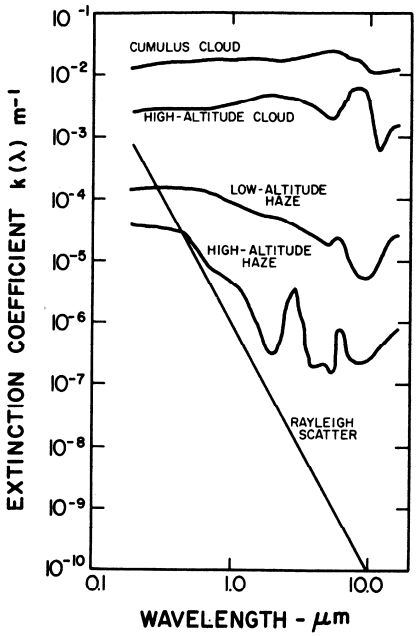

Figure 3.4. Aerosol extinction coefficient as a function of wavelength [Measures, 1992].

3.5.2 Ozone Correction for UV Water Vapor

Ozone absorbs wavelengths over a wide region between 200 nm and 300 nm in the Hartley band, and at wavelengths up to 340 nm in the Higgens band. The region between 200 nm and 300 nm is known as the "solar blind" portion of the ultra-violet spectrum. An advantage to operating in the solar blind portion of the spectrum is that the

stratospheric ozone helps block the high solar daytime radiance, thus allowing daytime lidar measurements. A disadvantage to operating in this region is the tropospheric ozone absorbs a portion of the incident radiation at 266 nm, and a portion of the Raman shifted return signals which leads to weaker return signals. During the day lidar measurements can only be taken in this region because of the intense visible background radiation at other wavelengths. Figure 3.4 displays the Hartley absorption band with the 1st Stokes vibrational Raman shift from the 4th harmonic of the Nd:YAG laser.

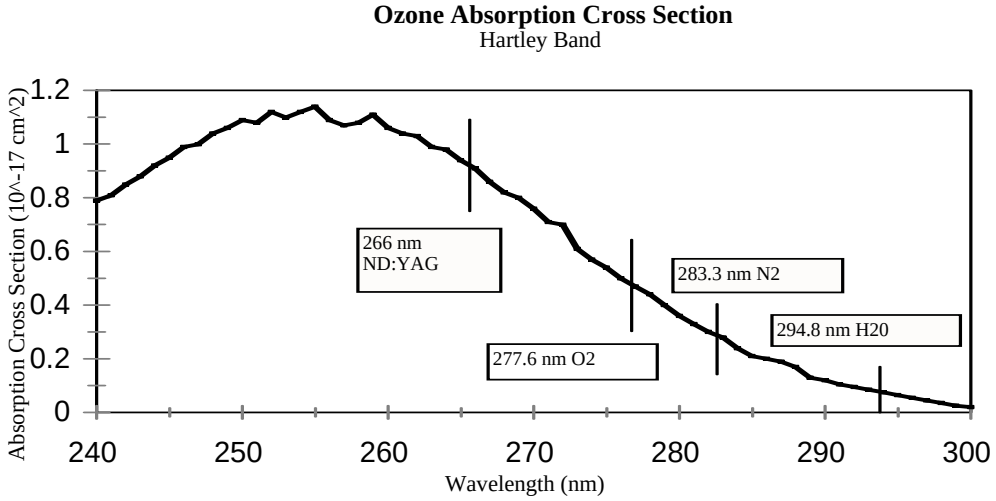

Figure 3.5. The Hartley band absorption cross-section of ozone is shown with the location of the wavelengths of the 4th harmonic of the ND:YAG laser and Raman shifted wavelengths for N_2, O_2, and H_2O are indicated.

Since the UV water vapor data is taken on the steep side of the Hartley absorption band, it becomes necessary to determine the ozone density in the measurement range. Taking the ratio of the oxygen and nitrogen return signals yields,

$$\frac{S_{O_2}(z)}{S_{N_2}(z)} = K \frac{N_{O_2}(z)}{N_{N_2}(z)} \exp\left[-\left(\sigma_{O_2} - \sigma_{N_2}\right) \int_0^z N_{O_3}(z')dz' \right] , \qquad (3.11)$$

where,

σ_{O2} is the absorption cross-section for O_3 at the Raman shifted wavelength,
σ_{N2} is the absorption cross-section for O_3 at the Raman shifted wavelength.

The wavelength dependence of the aerosol scattering between 284 and 277 nm has been neglected in this analysis. The ratio of $N_{O2}(z)$ to $N_{N2}(z)$ is constant through the lower atmosphere so Equation 3.11 can be solved to obtain the column density for ozone. Differentiating this equation yields a direct measure of ozone density $N_{O3}(z)$. Applying this to the UV water vapor mixing ratio yields,

$$w(z) = K \frac{S_{H_2O}(z)}{S_{N_2}(z)} \left(\frac{S_{O_2}(z)}{S_{N_2}(z)} \right)^{\frac{\sigma_{H2O} - \sigma_{N2}}{\sigma_{N2} - \sigma_{O2}}} , \qquad (3.12)$$

where σ are the absorption cross section values, which are 484.2 x 10^{-22} m^2 mol^{-1}, 285.4 x 10^{-22} m^2 mol^{-1}, and 79.9 x 10^{-22} m^2 mol^{-1}, for O_2, N_2, and H_2O respectively [Harris, 1996, also see Prasad and Mathur, 1998].

3.6 LAPS Measurement of Ozone

Originally, the Penn State Lidar group used the ozone measurement as a correction factor for the UV water vapor measurement. Then it was realized that if the

correction ratio was taken one step further, profiles of ozone could be provided. This can be seen in the following equation,

$$\frac{P_{O2}(z)}{P_{N2}(z)} = k_{system} * \exp\left[-\int_0^z [\alpha_m(\lambda_{O2,}\, z') - \alpha_m(\lambda_{N2,}\, z')]dz'\right] \exp\left[-\int_0^z [\alpha_{O3}(\lambda_{O2,}\, z') - \alpha_{O3}(\lambda_{N2,}\, z')]dz'\right]. \quad (3.13)$$

Equation 3.13 must again be corrected for molecular scattering at the two Raman shifted wavelengths as described in Section 3.5.1. The second exponential term, which was ignored for the visible water vapor, is due to the absorption due to ozone at the Raman shifted wavelengths. The expression is corrected for molecular scattering, and the integrated ozone number density in a specific scattering volume is solved for,

$$\int_0^z O_3(z')dz' = \ln\left(\frac{P_{O2}(z)}{P_{N2}(z)}\frac{1}{k_{System}}\right) * \frac{1}{(\sigma_{N2} - \sigma_{O2})} + \frac{(\sigma_{O2} - \sigma_{N2})}{(\sigma_{N2} - \sigma_{O2})} K(z). \quad (3.14)$$

Differentiating equation 3.14 over a scattering volume leads directly to the number of ozone molecules in that volume,

$$[O_3(z)] = \frac{d}{dz}\left[\ln\left(\frac{P_{O2}(z)}{P_{N2}(z)}\frac{1}{k_{System}}\right) * \frac{1}{(\sigma_{N2} - \sigma_{O2})} + \frac{(\sigma_{O2} - \sigma_{N2})}{(\sigma_{N2} - \sigma_{O2})} K(z)\right]. \quad (3.15)$$

where,

$[O_3(z)]$ is the number density of ozone in a scattering volume.

3.7 Error Analysis

The LAPS instrument uses photon counting photomultiplier tubes to collect data. Poisson statistics are used for the error analysis for the data collected. A Poisson distribution is generally appropriate for counting experiments where data represents the number of items observed per unit time interval. The Poisson distribution represents an approximation to the binomial distribution for the special case where the average number of successes is much smaller than the maximum possible number. This is true in this case since the number of photons collected is much less than the total number of photons scattered. The Poisson distribution is represented as,

$$P_p(x;\mu) = \frac{\mu^x}{x!} e^{-\mu} \tag{3.16}$$

where x represents the number of photons counted and μ is the mean value. In Poisson statistics, the expectation of x is equal to the mean value, and the standard deviation of x is equal to the square root of the mean value. The relative uncertainty is given by,

$$\frac{\sigma}{x} = \frac{\sqrt{\mu}}{x} = \frac{1}{\sqrt{x}} \ . \tag{3.17}$$

The LAPS instrument integrates each data channel for one minute in 75 meter range bins. A longer integration time is necessary for processing some of the parameters from the raw data. Propagation of error techniques must be used when combining data. The error associated with the signal does not just add. If two random variables x and y

each with standard deviations σ_x and σ_y are added or subtracted (i.e. z = x ± y) the associated error σ_z will be,

$$\sigma_z^2 = \sigma_x^2 + \sigma_y^2 \pm 2 r_{xy} \sigma_x \sigma_y \,, \tag{3.18}$$

where,

σ_x is the standard deviation of x,
σ_y is the standard deviation of y,
r_{xy} is the correlation between x and y,
σ_z is the standard deviation of the new variable z = x + y.

When channels are multiplied and divided to obtain the data output, the error must be propagated correctly. For example, if x and y are two separate measurements with standard deviations σ_x and σ_y, the product z = xy will have a standard deviation σ_z,

$$\frac{\sigma_z^2}{z^2} = \frac{\sigma_x^2}{x^2} + \frac{\sigma_y^2}{y^2} + 2\frac{r_{xy}\sigma_x\sigma_y}{xy} \tag{3.19}$$

The final case that needs to be address is when x and y are divided to form z = x / y, the associated standard deviation σ_z will be,

$$\frac{\sigma_z^2}{z^2} = \frac{\sigma_x^2}{x^2} + \frac{\sigma_y^2}{y^2} - 2\frac{r_{xy}\sigma_x\sigma_y}{xy} \tag{3.20}$$

In the studies for this thesis, it is assumed that r_{xy} is small compared to σ_x and σ_y and is thus neglected.

3.8 Optimal Estimation of Water Vapor

During nighttime measurements, the LAPS instrument obtains real time data from water vapor with both the visible and ultra-violet techniques described above. These measurements at each range bin have a value for water vapor with its associated standard deviation. The LAPS instrument combines these measurements optimally with a weighted average technique,

$$water_{opt} = \left(\frac{1}{\sigma vis} + \frac{1}{\sigma uv} \right)^{-1} \left(\frac{wat_{vis}}{\sigma vis^{2}} + \frac{wat_{uv}}{\sigma uv^{2}} \right) \tag{3.21}$$

$$\sigma_{water_{opt}} = \left(\frac{1}{\sigma vis} + \frac{1}{\sigma uv} \right)^{-\frac{1}{2}} \tag{3.22}$$

where,

$water_{opt}$ is the weighted average between the visible and ultra violet water vapor measurement,
$\sigma_{wateropt}$ is the standard deviation of the weighted average,
wat_{vis} is the visible water vapor measurement,
wat_{uv} is the ultra-violet water vapor measurement,
σ_{vis} is the standard deviation of the visible water vapor measurement,
σ_{uv} is the standard deviation of the ultra-violet water vapor measurement.

Chapter 4

Tropospheric Ozone and Water Vapor Measurements During the Southern California Ozone Study

4.1 Southern California Ozone Study

The PSU participation in the Southern California Ozone Study (SCOS) was co-sponsored by the California Air Resources Board (ARB), the Mojave Desert Air Quality Management District (MDAQMD), the USEPA National Exposure and Research Laboratory and the US Marine Corp at 29 Palms. The goal of the study was to develop databases that support detailed photochemical modeling and analysis to better understand the processes involved in the formation of high ozone concentrations in the South Coast Air Basin and across the southern California region [CARB, 1999].

The Penn State University field measurement activity in the SCOS program was undertaken to investigate the process leading to ozone production in the Los Angeles basin and subsequent transport into the high desert that lies to the east. The instrument was co-located at a site with a Radio Acoustic Sounding System (RASS) instrument and a meteorological station, operated by Radian International Corporation located in Hesperia CA. The RASS instrument was operated by SONOMA Technology Inc. This site was located in the high desert near the top of the Cajon Pass and was chosen because the area of the Cajon Pass is believed to be a major passageway for ozone from Los Angeles into the high desert. Figure 4.1 shows the geographical location of the site in Hesperia with respect to Los Angeles.

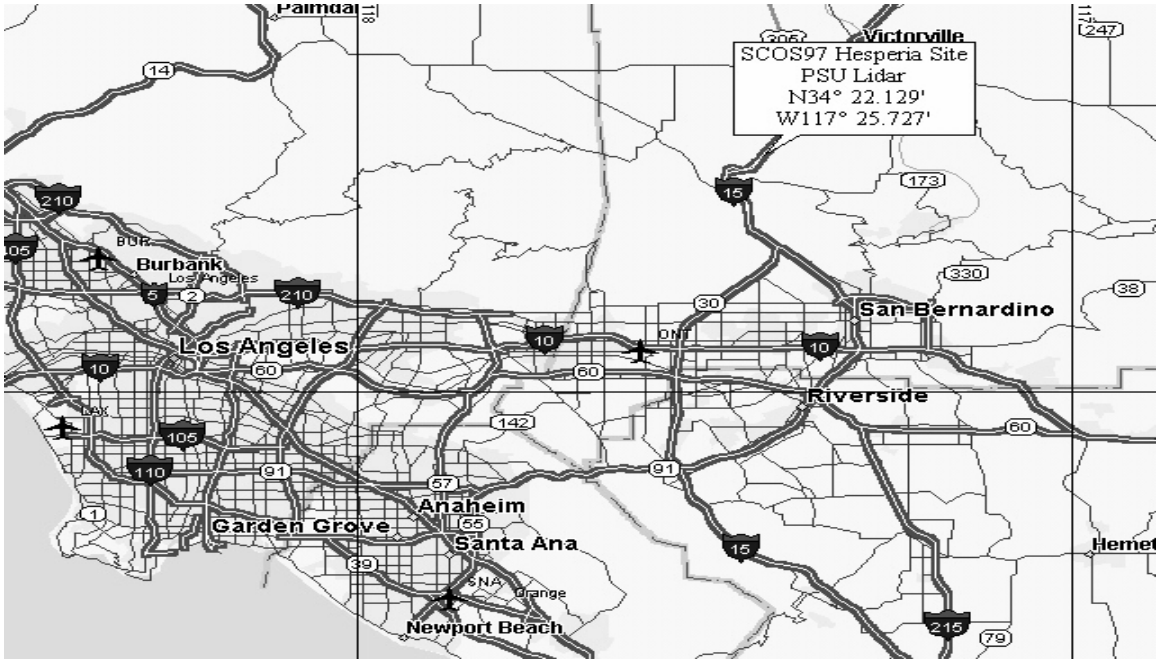

Figure 4.1 A map of Southern California illustrating the geographical position of the Hesperia site with respect to Los Angeles.

During the SCOS campaign the LAPS instrument collected data for nearly 10 hours per day from 29 August through 19 September 1997. LAPS was just one of the many instruments that collected atmospheric data. Three sets of LAPS lidar instrument measurements were coordinated with measurements from aircraft operated by the University of California, Davis. On the 18th and 19th of September, the aircraft performed ascending and descending flights which approximately mapped the sides of a 2 km square box centered on the lidar beam. Each ascent or descent took approximately 15 minutes. Radiosonde balloons were also launched at the Hesperia Site by Penn State to establish and verify the calibration constants for water vapor and temperature profile analysis.

4.2 Data Correction

During the initial data processing for the SCOS campaign, it was noticed that the low altitude data measurements obtained from the ultraviolet wavelengths were not consistent with the aircraft data. The low altitude ozone data was consistently larger than the aircraft data. Also, the water vapor measurements obtained from the ultraviolet and visible wavelengths did not compare well at low altitudes. The water vapor measurements usually track each other unless sulfur dioxide or some other chemical substance, which absorbs ultraviolet radiation, is in the air. Further analysis of the data revealed that the visible water vapor data compared well with the aircraft data and weather balloons launched during the SCOS campaign.

Up until this point, the LAPS instrument had compared well with other instruments that measured the same properties. Analysis of the performance led to the conclusion that the problem with the ultraviolet data was due to vignetting somewhere in the optical path in the detector box. Vignetting is the unintended shadowing of ray paths passing through an optical instrument [Hecht, 1990]. It is believed that the ultraviolet light in the detector box was being clipped at the periphery of the beam. The low altitude was the most affected since the backscattered light in this region enters at a different range of modes of the optical fiber and this results in a changing beam diameter. A larger beam diameter causes the light to be clipped at its peripheries by one or more of the components in the detector box. The effect was amplified in the ozone profiles since ozone density is obtained by differentiating the ratio of the return signal. Any small differences in the return signals due to vignetting are amplified due to the process of taking the derivative of the original profile. Figures 4.2 a and 4.2 b show a comparison

on two separate days of ozone profiles from the LAPS instrument and the aircraft data, illustrating the problem with the low altitude ozone data. The LAPS data was integrated for 30 minutes centered around the 15 minute ascent or descent of the aircraft.

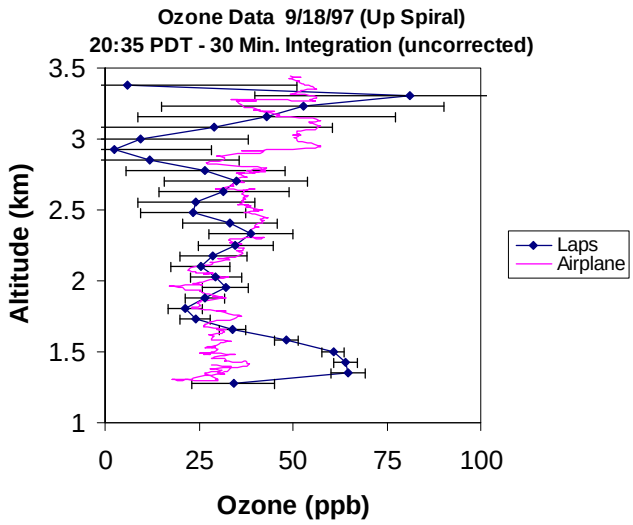

Figure 4.2 (a). A comparison of ozone data from the LAPS instrument and the University of California, Davis aircraft from 18 September 1997 which demonstrates the low altitude vignetting problem. The altitude of the site was 1167 meters.

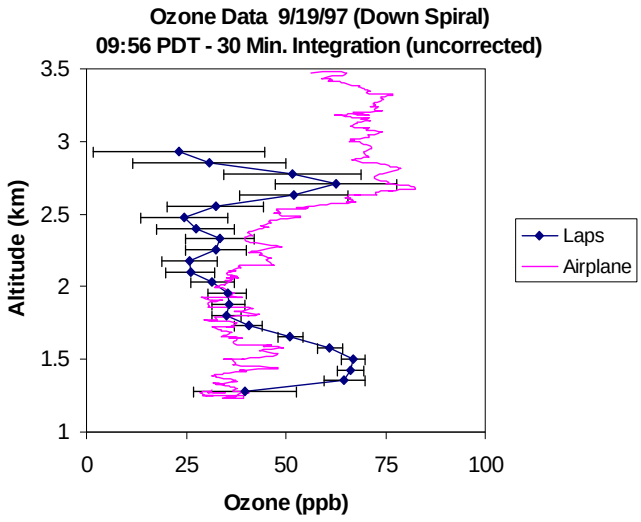

Figure 4.2 (b). A comparison of ozone data from the LAPS instrument and the University of California, Davis aircraft from 19 September 1997 which demonstrates the low altitude vignetting problem.

4.2.1 Vignetting Correction

A correction for the ultraviolet data had to be derived after the instrument returned from California. If the problem had been detected while the instrument was still on site, vignetting data could have been obtained to permit correction of the raw data before it was processed. Since this was not the case, a correction was derived using the aircraft ozone data and the water vapor data from the LAPS instrument.

The visible water vapor data was considered to be correct since it compared well with the aircraft data and radiosonde balloon data obtained during the campaign. The ultraviolet water vapor data was obtained from the lidar raw data by taking the ratio of H_2O to N_2, and then correcting for integrated ozone by using the ratio of O_2 to N_2 (Equation 3.12). This can be written as,

$$w_{uv}(z) = K \frac{S_{295}(z)}{S_{284}(z)} \left(\frac{S_{277}(z)}{S_{284}(z)} \right)^{1.034} \tag{4.1}$$

where,

S_{295} is the Raman shifted return signal from H_2O at 295 nm,
S_{284} is the Raman shifted return signal from N_2 at 284 nm,
S_{277} is the Raman shifted return signal from O_2 at 277 nm,
K is a calibration constant.

The exponent value of 1.034 is the correction for the ultraviolet water vapor due to ozone absorption. This value is derived from the ratio of the Hartley band cross sections for the various wavelengths.

The ratio of visible to ultraviolet water vapor data provided information about the total vignetting in the ultraviolet water vapor measurement. The vignetting was present in both the 295 to 284 nm ratio and in the 277 to 284 nm ratio data. The ratio of the

visible to ultraviolet water vapor data was obtained at sixteen different times during the SCOS campaign. The data was integrated for 30 minutes, then the ratio of the two measurements was taken. The average of the ratios with the associated ±1σ standard deviation can be seen in Figure 4.3. The solid line represents a fit through the data points and was used as a measure of the total vignetting in the ultraviolet water vapor data.

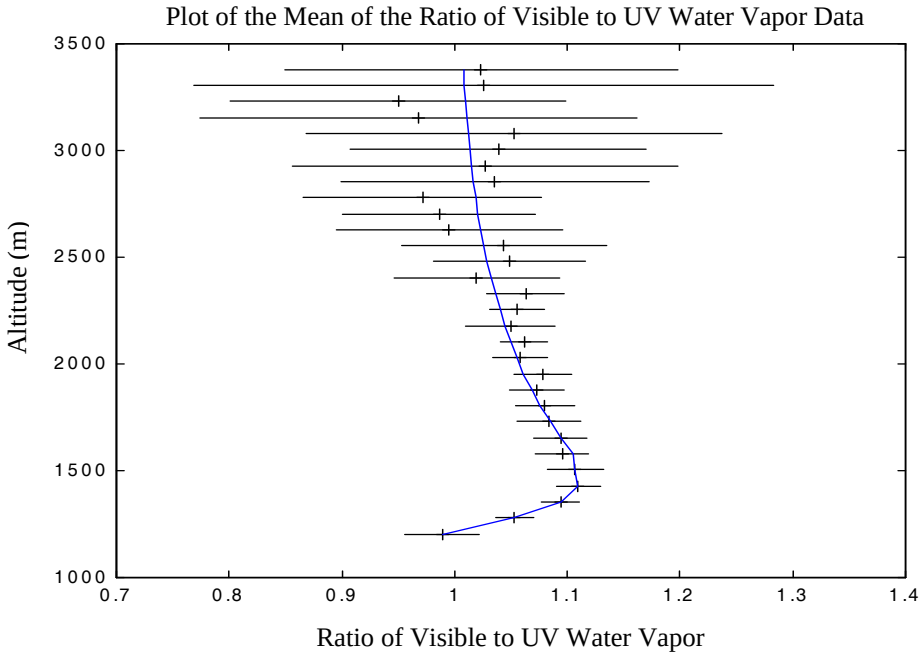

Figure 4.3. Plot of the mean of the ratio of visible to ultraviolet water vapor data for 16 cases with its associated ±1σ standard deviation. The solid line is a smoothed best fit through the data points.

The total effect of vignetting and ozone absorption in the ultraviolet water vapor data was obtained from the ratios to the visible data, which was assumed to be correct. The aircraft ozone data was used to determine the vignetting in the 277/284 ratio. An iterative program was written that muliplied the 277/284 raw data ratio, below 1 km and at each 75 m bin, by a number which was slightly larger or smaller than 1. The initial

value of this multiplication factor at each bin was set to 1. The values were varied until the ozone data below 1 km was equal to the aircraft data. The correction term approached unity as the altitude approached 1 km as expected because the return signal is focused at and above this altitude. Figure 4.4 shows the vignetting correction curve derived from the aircraft data for the 277/284 raw data ratio. This curve was applied to the 277/284 raw data ratio before processing.

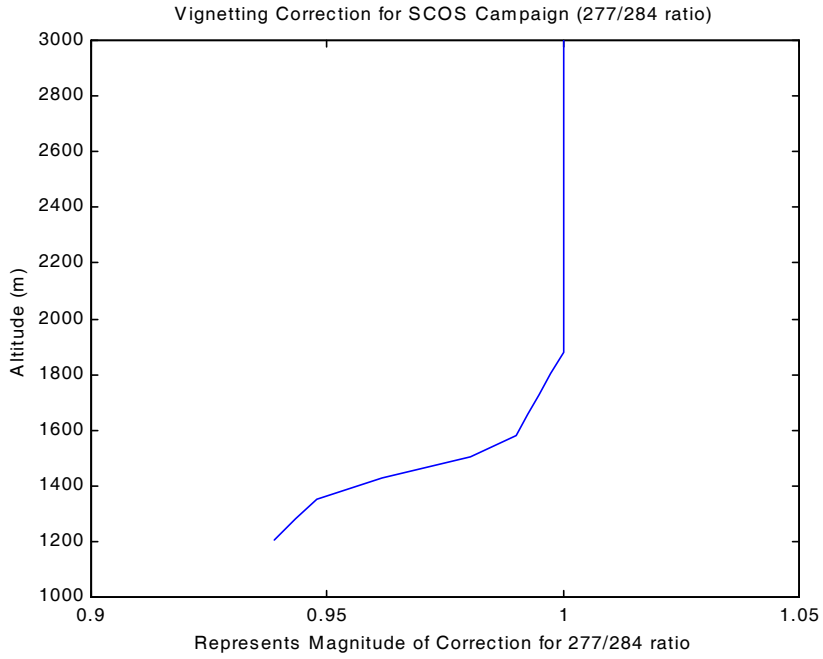

Figure 4.4. Vignetting correction for the 277/284 raw data ratio of O_2/N_2.

The vignetting correction for the 295/284 ratio (Figure 4.3) was found analytically using the shape of the vignetting correction profile derived for the 277/284 ratio scaled to the total vignetting in the ultraviolet water vapor data. The total vignetting in the ultraviolet water vapor data can be written as,

$$totalvignw_{uv}(z) = vigncorH_2O(z)\left(vigncorO_2(z)\right)^{1.034} . \quad (4.2)$$

Solving for the 295/284 vignetting correction ratio,

$$vigncorH_2O(z) = totalvignw_{uv}(z)\left(vigncorO_2(z)\right)^{-1.034} \quad (4.3)$$

where,

vigncorH₂O is the vignetting correction curve for the 295/284 raw data ratio,
vigncorO₂ is the vignetting correction curve for the 277/284 raw data ratio.

Equation 4.3 was solved for the vignetting correction for the 295/284 raw data ratio. Figure 4.5 shows the vignetting correction curve derived for the 295/284 raw data ratio which must be applied to the raw data ratio before processing.

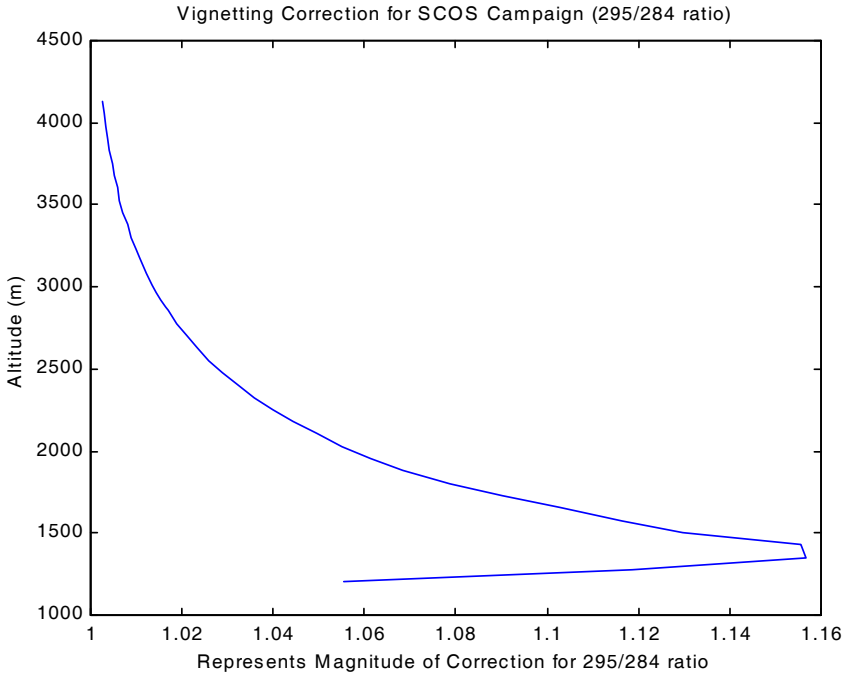

Figure 4.5 Vignetting correction for the 295/284 ratio.

The vignetting correction curve is applied as a multiplication factor at each bin to the raw data ratio of the ultraviolet wavelengths. This data correction was derived assuming that the visible water vapor data obtained with the LAPS instrument and the ozone data obtained with the aircraft from University of California at Davis aircraft are correct, and assuming also that vignetting was the source of all differences between these sets of profiles.

Since the SCOS campaign, the Penn State EE/ARL lidar group has developed a systematic way to correct for vignetting. The technique will briefly be explained for the ultraviolet channels but could also be applied to the visible channels if needed. A model of the vignetting in the ultraviolet channels can be experimentally obtained by placing a 277 nm narrow band pass filter in each of the ultraviolet channels. With the same filter in each channel, a constant ratio should exist when taking the ratio of two channels. Instead a constant ratio is found for data approximately 1 km above ground level. The deviation from the constant, which was found at altitudes lower than 1 km, is due to vignetting. The ratio above 1 km is averaged and the vignetting model is divided by this average to normalize the points above 1 km. The raw data above 1 km will be unchanged when the vignetting correction is applied to the ratio. The vignetting model is then inverted and applied as a correction to the raw data ratios. The real time processing of the LAPS instrument has been modified to accept normalized vignetting data calibrations. It has also been modified to add the error associated with the vignetting correction with propagation of error techniques. It is essential to take vignetting data calibration runs whenever the LAPS instrument is moved from one location to another because of the possible change in the optical alignment. Vignetting testing should be accomplised at the

beginning of each campaign so that the real time data output is tested and if necessary corrected for vignetting.

4.3 Water Vapor and Ozone Data

After the raw data ratios were corrected for vignetting, the LAPS ozone data compared well with the aircraft data. The same plots of ozone that were shown in Figures 4.2 (a) and 4.2 (b), for 18 and 19 September, 1997, are again shown in Figures 4.6 (a) and 4.6 (b). The ozone data in these figures have been corrected for vignetting. The correction in the raw data ratio (277/284 nm) was 6% at its maximum and corresponds to a correction in ozone of 50 ppb. Figures 4.6 (c) and 4.6 (d) are water vapor profiles comparing the LAPS instrument with the aircraft data from 18 and 19 September, 1997. The LAPS data was integrated for 30 minutes centered about the time of ascent or descent of the plane. These measurements also compare well.

One of the most valuable tools used to examine variations in the atmosphere are time sequence plots. Several graphical user interface programs have been written to manipulate and smooth data. Monitoring water vapor with a time sequence plot gives valuable information about the net convective mixing present in the atmosphere and can also help predict what to expect in terms of the dynamics of the atmosphere. The time sequences of ozone are also valuable because they can be used in conjuction with other data to predict when high ozone events may occur.

Figures 4.7 (a) and 4.7 (b) show time sequences of ozone and water vapor, respectively, for 5 September, 1997. The time sequence of ozone is integrated for 30 minutes with 5 minute steps, and is clipped at the top when the error bar is greater than or

equal to 35% of the signal. The time sequence of water vapor is integrated for 5 minutes with 1 minute steps, and is clipped at the top when the error is greater than or equal to 25% of the signal. The time sequence of ozone shows the levels of ozone, between 17:30 and 19:00, approaching the 120 ppb health safety limit set by the EPA. The time sequence of water vapor reveals an increase in the water vapor mixing ratio at the same time. The measurements show a plume of polluted air that has transported both moisture and ozone. The plume of air containing ozone and water vapor may have been transported from Los Angeles through the Cajon pass. The other measurements from the campaign will be useful to analyze the transport and interpret the results.

Figures 4.8 (a) and 4.8 (b) are also time sequences of ozone and water vapor, respectively, for 17 September, 1997. The time sequence of ozone is integrated for 30 minutes with 5 minute steps, and is clipped at the top when the error is greater than or equal to 35% of the signal. The time sequence of water vapor is integrated for 5 minutes with 1 minute steps, and is clipped at the top when the error bar is greater than or equal to 25% of the signal. Again, it seems as if an ozone plume has been transported through the Cajon pass out into the high desert. In this case, the water vapor and ozone profile variations again exhibit a strong correlation which indicates that a plume of polluted air has been advected past our site between 1200 and 2145 PDT.

During this campaign, the LAPS instrument did not obtain data showing the formation or destruction of ozone in this region. Most likely, all ozone data obtained was from ozone that was generated at the surface in Los Angeles, then vertically mixed up above the atmosphere boundary layer and transported horizontally. Each air parcel was

transported horizontally from the Los Angeles area through the Cajon Pass and into the high desert.

4.3.1 Smoothing of Water Vapor Data

When analyzing a time sequence plot, it is important to separate what is real and what is an artifact of processing. The water vapor data is integrated for five minutes with one minute steps. If there is a bad point in one of those minutes of data, it will spread out over five minutes when it is integrated. Also, at the upper altitudes, the ultraviolet water vapor data is much noisier than the visible data due to extinction of the signal due to the $1/\lambda^4$ molecular scattering cross section dependence of the signal. The extinction due to molecular scattering at 266 nm is 16 times greater than that of the visible signal at 532 nm and the return signal is increased by the same factor. The UV signal at the lower altitudes is at times larger than the visible signal; however, the challenge is to smooth the upper altitude UV water vapor data to extend the daytime measurement altitude. An option to smooth data is available in the processing programs. Figures 4.9 (a) and 4.9 (b) are the same time sequences of water vapor shown in Figures 4.8 (a) and 4.8 (b). Smoothing has been applied to these time sequences to aid in removing the artifacts of processing. The smoothing algorithm that was applied here takes a point and averages it with 2 points above and below it in altitude. It then takes the same point and averages it with two points before and after it in time. Propagation of error techniques are then used to obtain the associated error. Smoothing can remove real factors in the atmosphere, such as wave variations and turbulent cells, so it is useful to examine both the smoothed and unsmoothed data sets.

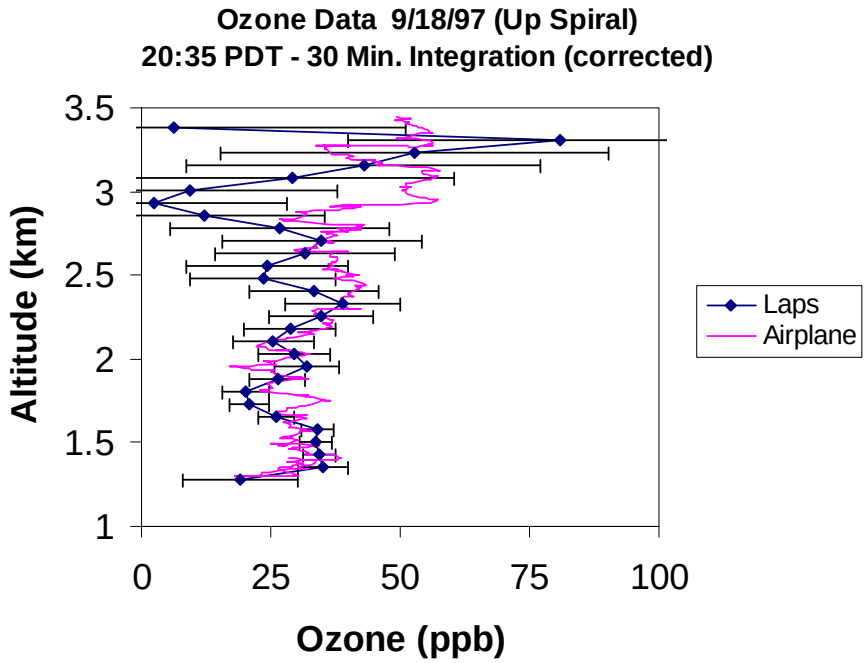

Figure 4.6 (a). A comparison of ozone data from the LAPS instrument and the aircraft of the University of California at Davis from 18 September 1997.

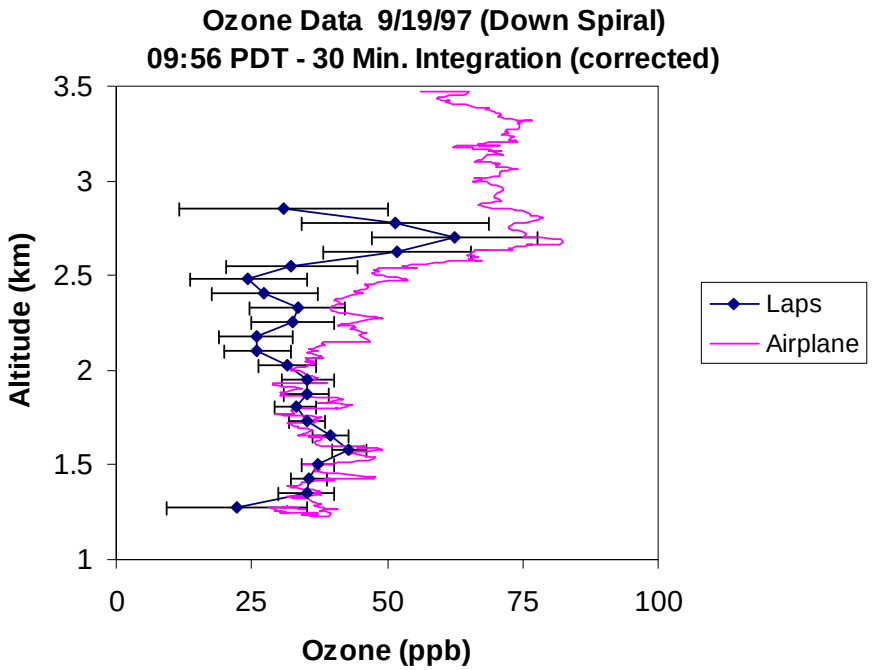

Figure 4.6 (b). A comparison of ozone data from the LAPS instrument and the aircraft of the University of California at Davis from 19 September 1997.

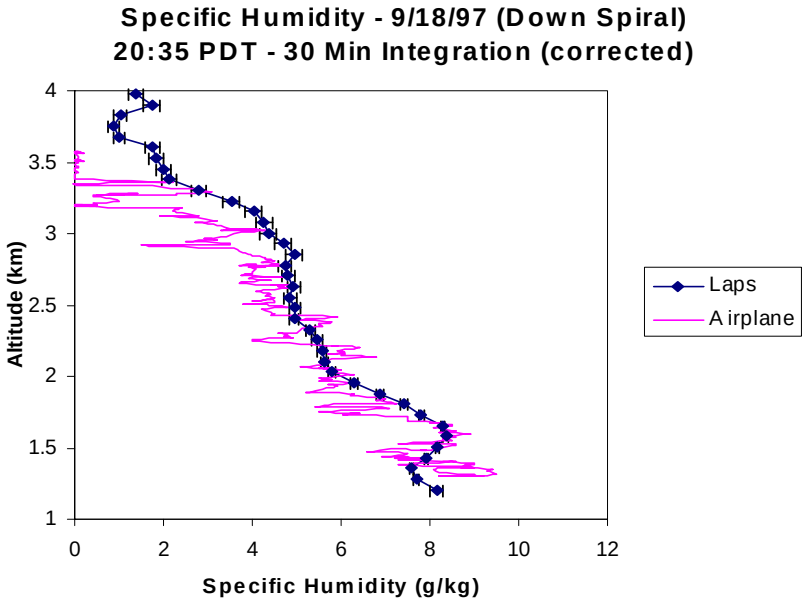

Figure 4.6 (c). A comparison of water vapor data from the LAPS instrument and the aircraft of the University of California at Davis from 18 September 1997.

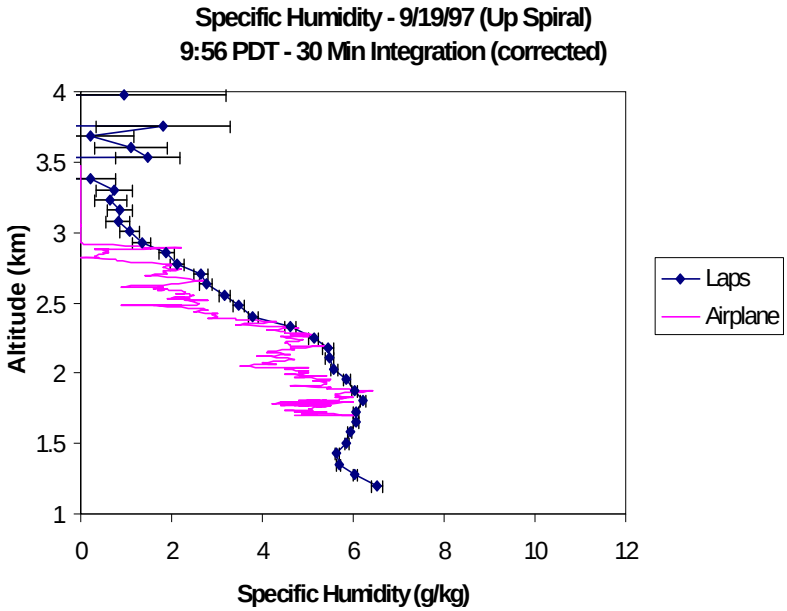

Figure 4.6 (d). A comparison of water vapor data from the LAPS instrument and the aircraft of the University of California at Davis from 19 September 1997.

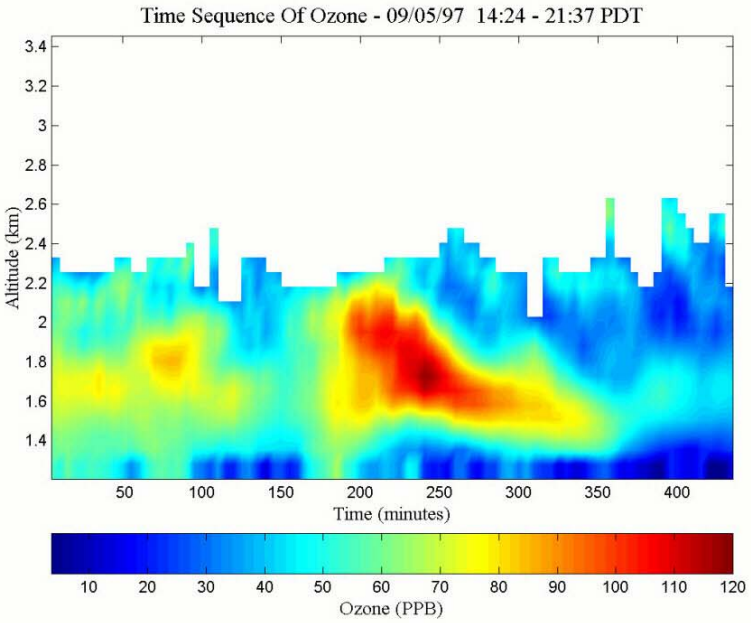

Figure 4.7 (a). Time sequence of ozone density from 5 September, 1997.

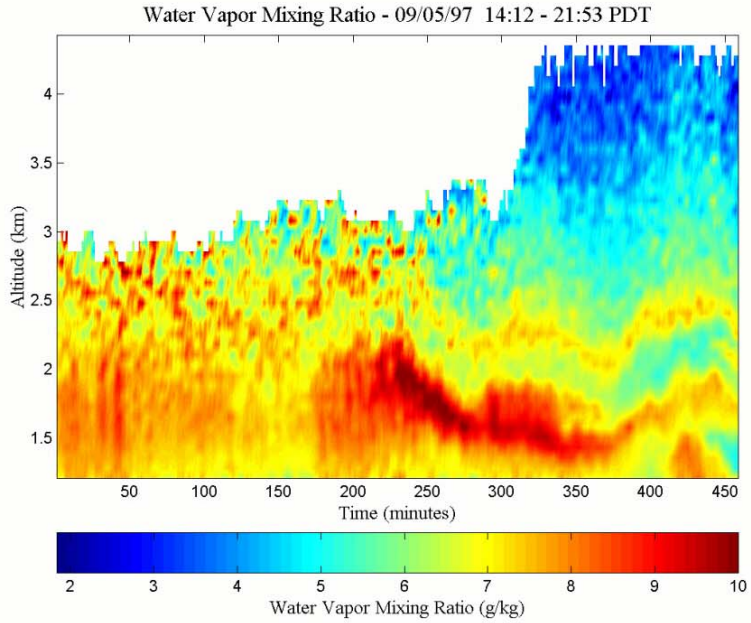

Figure 4.7 (b). Time sequence of water vapor mixing ratio from 5 September, 1997.

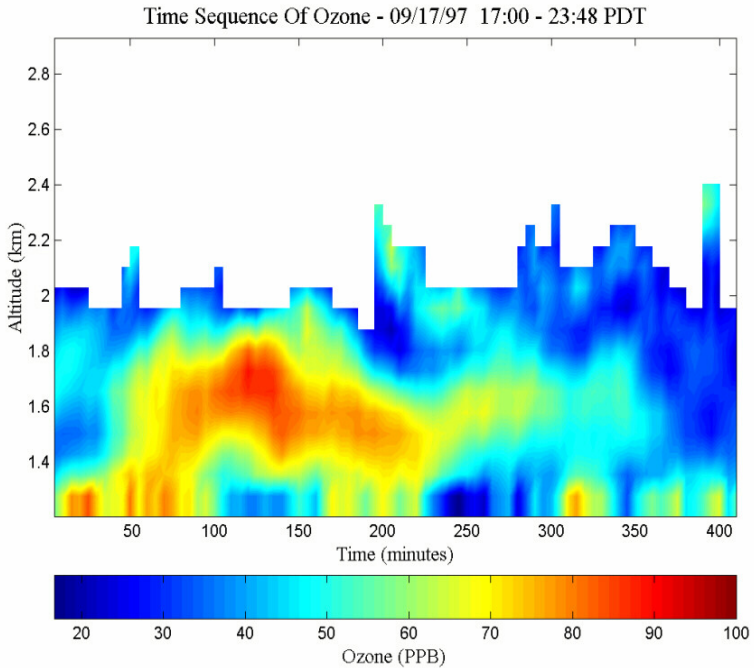

Figure 4.8 (a). Time sequence of ozone density from 17 September, 1997.

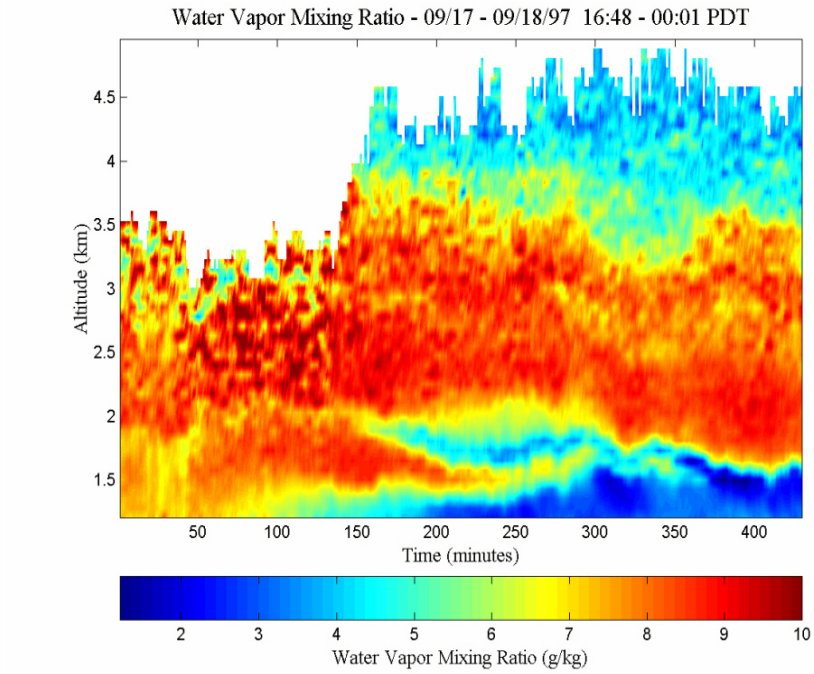

Figure 4.8 (b). Time sequence of water vapor mixing ratio from 17 September, 1997.

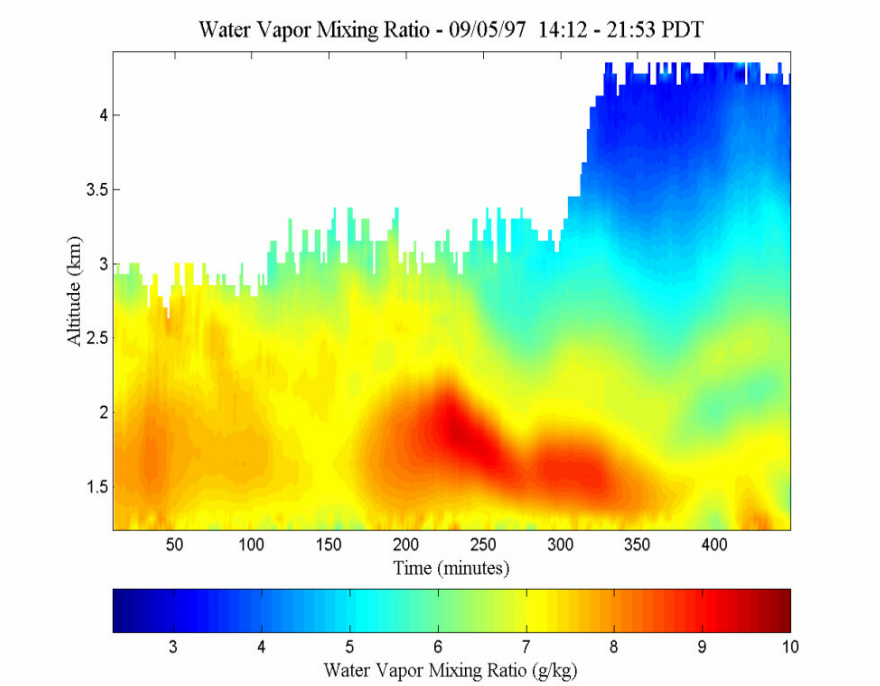

Figure 4.9 (a). Time sequence of water vapor mixing ratio from 5 September, 1997 with smoothing applied.

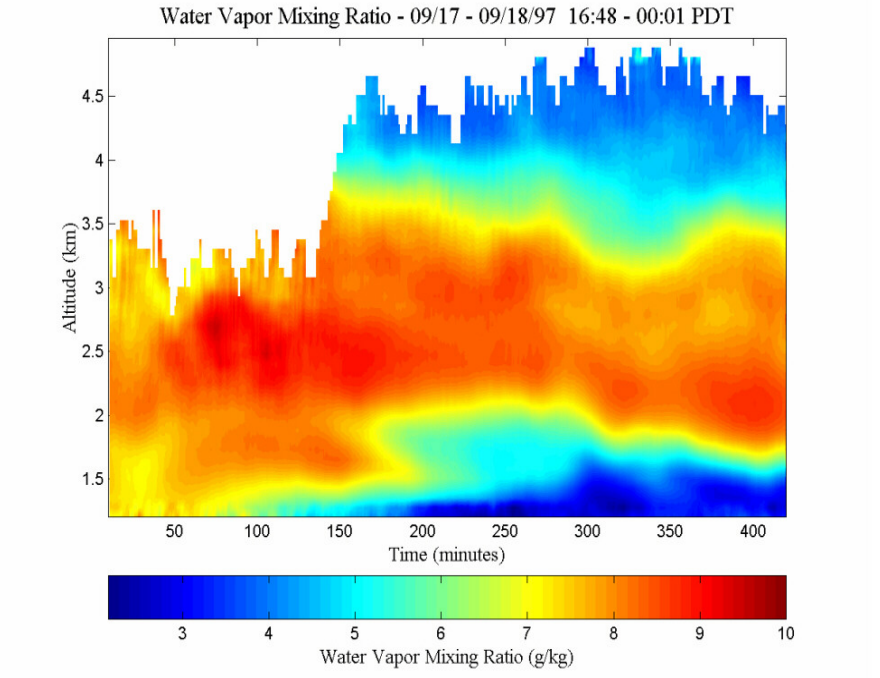

Figure 4.9 (b). Time sequence of water vapor mixing ratio from 17 September, 1997 with smoothing applied.

Chapter 5

Conclusions

Tropospheric ozone is toxic to life on earth and needs to be monitored continuously. The monitoring of this substance has to be performed frequently enough to distinguish between the short-term variations of tropospheric ozone due to pollution sources and meteorological events that transport and concentrate ozone in the troposphere. Several instruments have been developed to measure this toxic substance. More recently, the focus has been on the transport of tropospheric ozone and the fine particles that form ozone with a photochemical reaction. Water vapor and extinction measurements can aid in characterizing and modeling the transport of ozone and its precursors.

The LAPS lidar instrument can simultaneously measure atmospheric properties, and the real time profiles, of ozone, water vapor, temperature, and extinction (both molecular and aerosol). The measurements are range resolved in 75 m bins. The time resolution is 5 minutes for water vapor and 30 minutes for ozone, temperature, and extinction. This instrument has the time resolution necessary to monitor and model these processes.

Results collected during the Southern California Ozone Study were presented. The results show that the LAPS lidar instrument is capable of measuring atmospheric properties of ozone and water vapor in the troposphere accurately. When the LAPS data was compared with the University of California, Davis aircraft data, it compared well.

A vignetting correction has been developed and will be applied to the data as needed. Smoothing algorithms have been examined to manipulate and filter the data.

References

Bevington, P. R., and D. K. Robinson, *Data Reduction and Error Analysis For The Physical Sciences*. New York: McGraw-Hill inc., 1992.

California Air Resources Board (CARB). *Southern California Ozone Study–NARSTO* [WWW document]. URL http://www.arb.ca.gov/research/scos/scos.htm

Durbin, W. A., "Lidar Measurements of Ozone in the Lower Atmosphere," Masters Thesis, The Pennsylvania State University, Department of Electrical Engineering, December 1997.

Electrical Power Research Institute (EPRI) pamphlet, "Ozone: One Gas, Two Environmental Issues," Proceedings of the EPRI Environmental Briefing, Palo Alto, California, Dec 1988.

Environmental Protection Agency (EPA), *Atmospheric Observations: Helping Build The Scientific Basis For Decisions Related to Airborne Particulate Matter*, Report of the PM Measurements Research Workshop, Chapel Hill, North Caroline, July 1998.

Environmental Protection Agency (EPA) (n.d. / 1999). *Ozone: Good Up High, Bad Nearby* [WWW document]. URL http://www.epa.gov/oar/oaqps/gooduphigh

Esposito, S. T. and C. R. Philbrick, “Raman / DIAL Technique for Ozone Measurement,” Proceedings of the Nineteenth International Laser Radar Conference, NASA Langley Research Center, Hampton, VA, NASA Conf. Publ. 207671, pp. 407 - 410, July 1998

Harris, R S., "Observations of Atmospheric Water Vapor Using Raman Lidar Techniques" Masters Thesis, The Pennsylvania State University, Department of Electrical Engineering, May 1996.

Hecht, E., *Hecht Optics Second Edition*. Massachusetts: Addison-Wesley Publishing Company, 1990.

Hidy, G. M., P. M. Roth, J. M. Hales, and R. Scheffe, "Oxidant Pollution and Fine Particles: Issues and Needs," Journal of Air and Waste Management, June 1998.

Jenesse, J. R., Jr., D. B. Lysak, Jr. and C. R. Philbrick, "Design of a lidar receiver with fiber-optic output," Applied Optics 18, 4278 - 4284, 1997.

Liou, K. N., *An Introduction to Atmospheric Radiation*. California: Academic Press Inc., 1980.

Lyons, T. J. and W. D. Scott, *Principles of Air Pollution Meteorology*. Florida: CRC Press, Inc., 1990.

USSA76, National Oceanic And Atmospheric Admistration (NOAA), National Aeronautics and Space Administration (NASA), United State Air Force (USAF*), U. S. Standard Atmosphere, 1976*, Washington D. C., U. S. Government Printing Office, 1976.

Measures, R. M., *Laser Remote Sensing*. New York: John Wiley & Sons, 1992.

Papoulis, A., *Probability, Random Variables, and Stochastic Processes 3rd Edition*, New York: McGraw-Hill, 1991.

Philbrick, C. R. and D. B. Lysak, Jr., "Optical Remote Sensing of Atmospheric Properties," Proceedings of the Battlespace Atmospheric and Cloud Impacts on Military Operations, Hanscom Air Force Base, MA, December 1998.

Philbrick, C. R. and D. B. Lysak, Jr., "Measurement Capabilities of the LAPS Lidar," Proceedings of the Battlespace Atmospheric Conference, San Diego, CA, December 1997.

Piexoto, J. P. and A. H. Oort, *Physics of Climate*. New York: American Institute of Physics, 1992.

Prasad, C. R. and S. Mathur, "A Compact Water Vapor Raman Lidar," Proceedings of the Nineteenth International Laser Radar Conference, NASA Langley Research Center, Hampton, VA, NASA Conf. Publ. 207671, pp. 371 - 3744, July 1998.

Schloerer, J., (1997, April). *Climate Changes: Some Basics* [WWW document]. URL http://www.lib.ox.ac.uk/internet/news/faq/archive/sci.climate-change.basics.html

Stevens, T. D., "An Optical Detection System for a Rayleigh/Raman LIDAR", Masters Thesis, The Pennsylvania State University, Department of Electrical Engineering, August 1992.

Walcek, C. J. and H. H. Yuan, "Calculated Influence of Temperature-Related Factors on Ozone Formation Rates in the Lower Troposphere," Journal of Applied Metorology, October 1994.

Wayne, R. P., *Chemistry of the Atmosphere 2nd Edition*, New York, Oxford University Press, 1991.

Appendix A

SCOS Campaign Results

This section contains profiles not given in Chapter 4 comparing the aircraft and the LAPS data that was corrected for vignetting. The LAPS data was integrated for 30 minutes centered around the ascent or descent of the aircraft.

Ozone Data

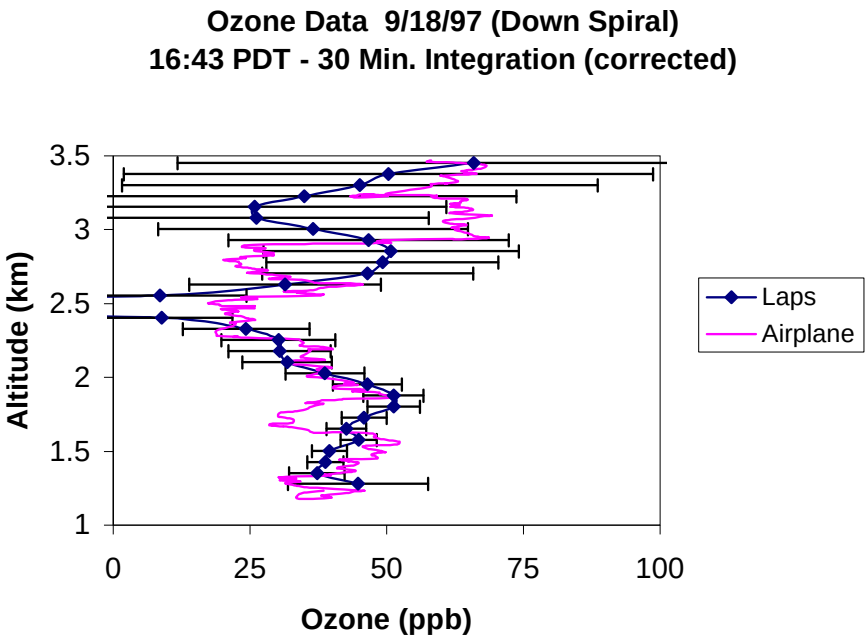

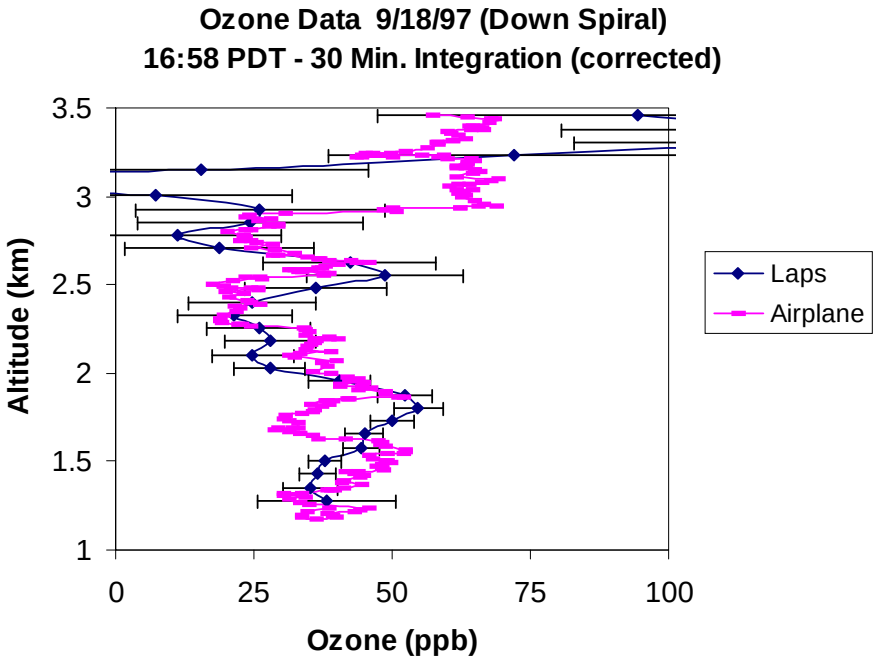
Ozone Data 9/18/97 (Down Spiral)
16:58 PDT - 30 Min. Integration (corrected)
Altitude (km)
3.5
3
2.5
2
1.5
1
0
25
50
75
100
Ozone (ppb)
Laps
Airplane

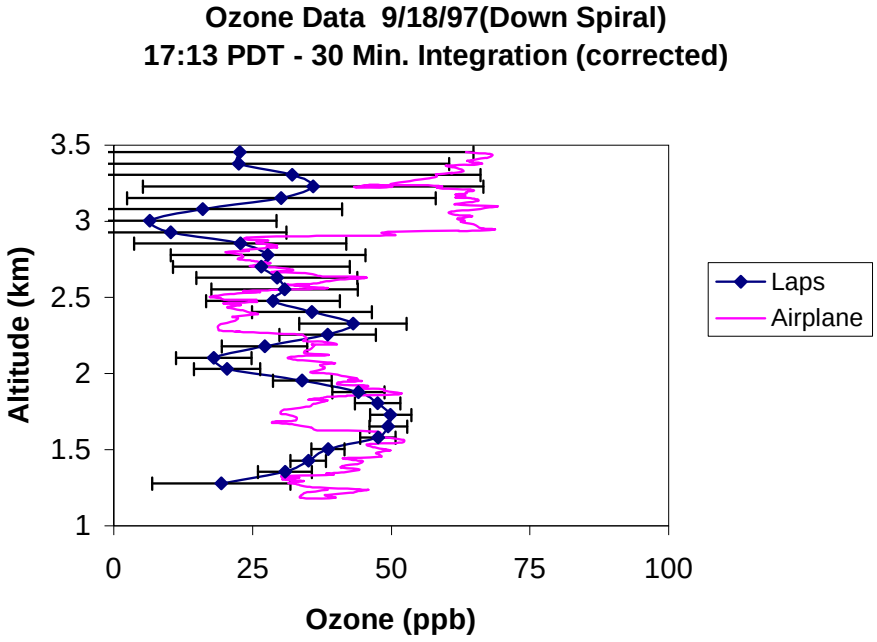
Ozone Data 9/18/97(Down Spiral)
17:13 PDT - 30 Min. Integration (corrected)
Altitude (km)
3.5
3
2.5
2
1.5
1
0
25
50
75
100
Ozone (ppb)
Laps
Airplane

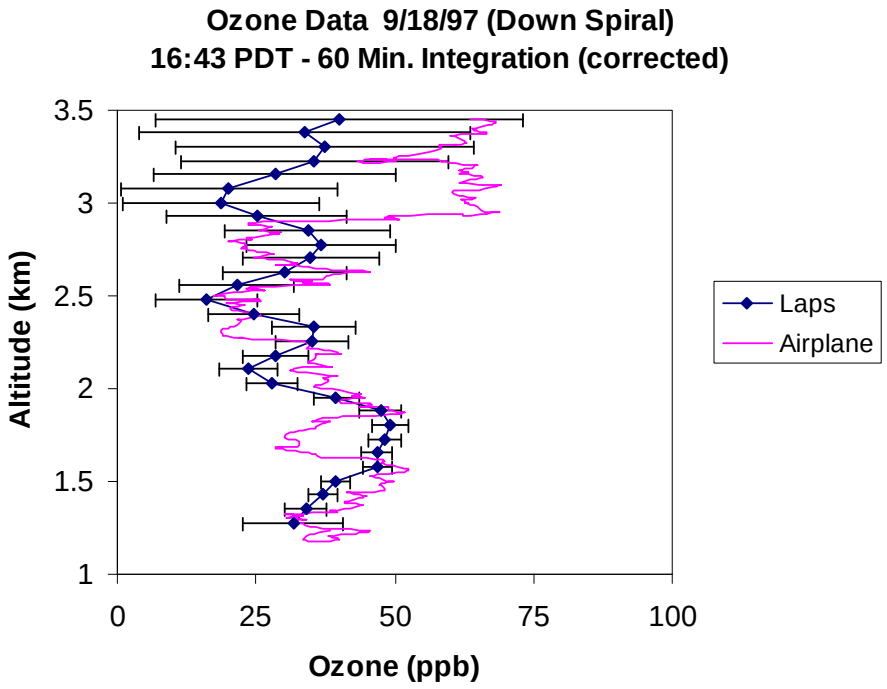
Ozone Data 9/18/97 (Down Spiral)
16:43 PDT - 60 Min. Integration (corrected)
Altitude (km)
3.5
3
2.5
2
1.5
1
0
25
50
75
100
Ozone (ppb)
Laps
Airplane

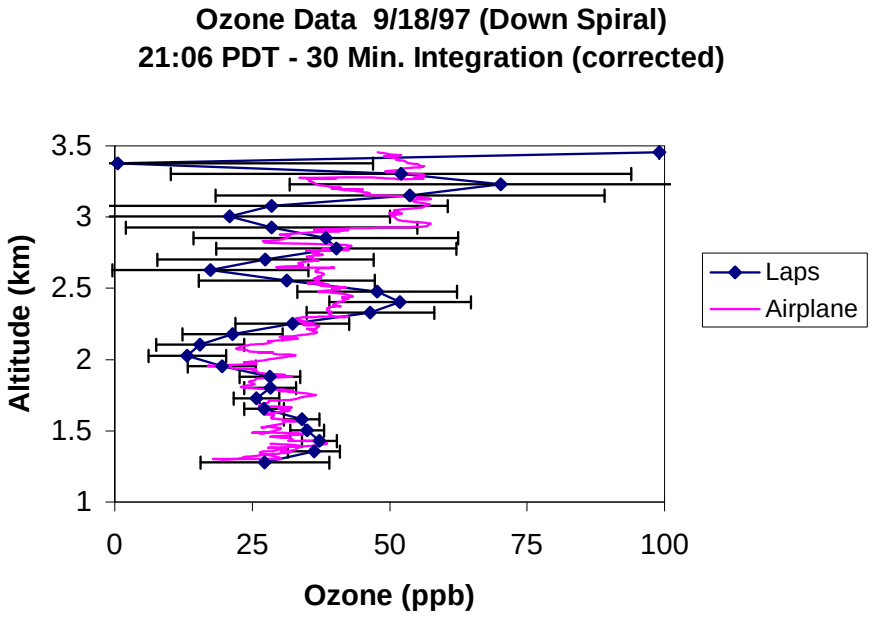
Ozone Data 9/18/97 (Down Spiral)
21:06 PDT - 30 Min. Integration (corrected)
Altitude (km)
3.5
3
2.5
2
1.5
1
0
25
50
75
100
Ozone (ppb)
Laps
Airplane

Ozone Data 9/18/97 (Up Spiral)
20:35 PDT - 30 Min. Integration (corrected)

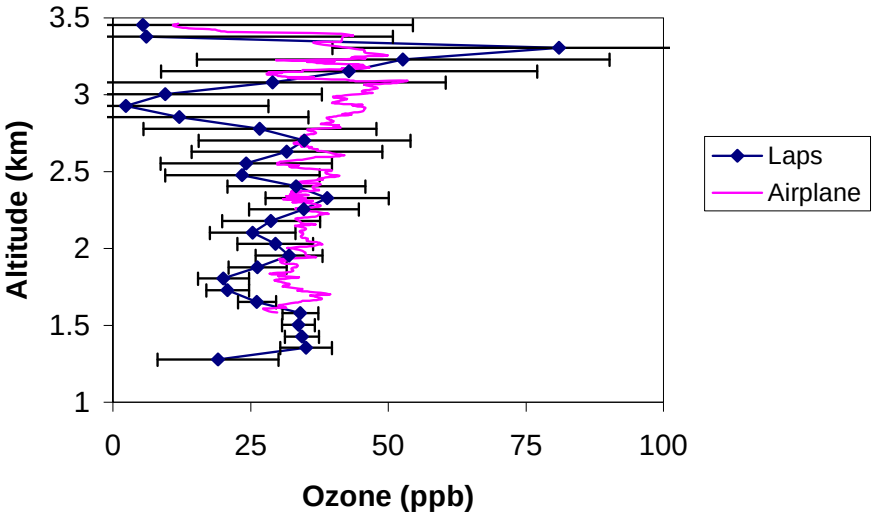

Ozone Data 9/18/97 (Up Spiral)
21:06 PDT - 30 Min. Integration (corrected)

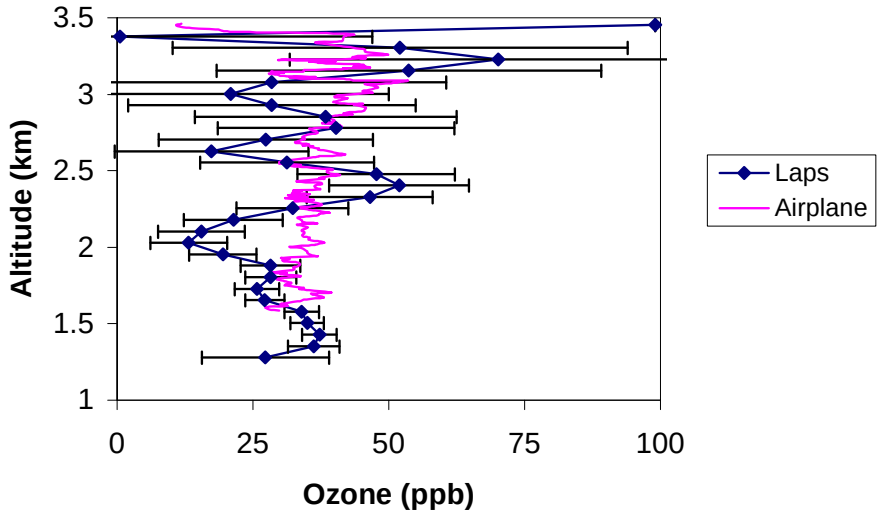

Ozone Data 9/19/97 (Up Spiral)
09:56 PDT - 30 Min. Integration (corrected)

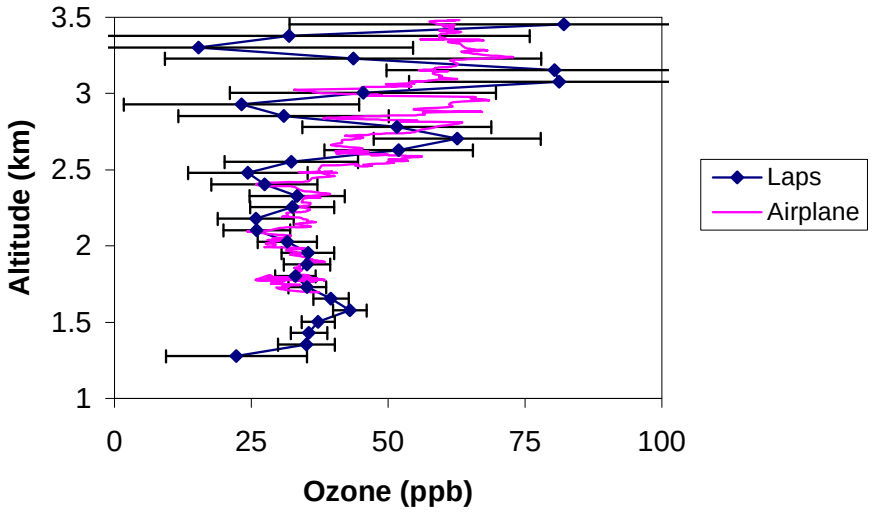

Ozone Data 9/19/97 (Up Spiral)
10:27 PDT - 30 Min. Integration (corrected)

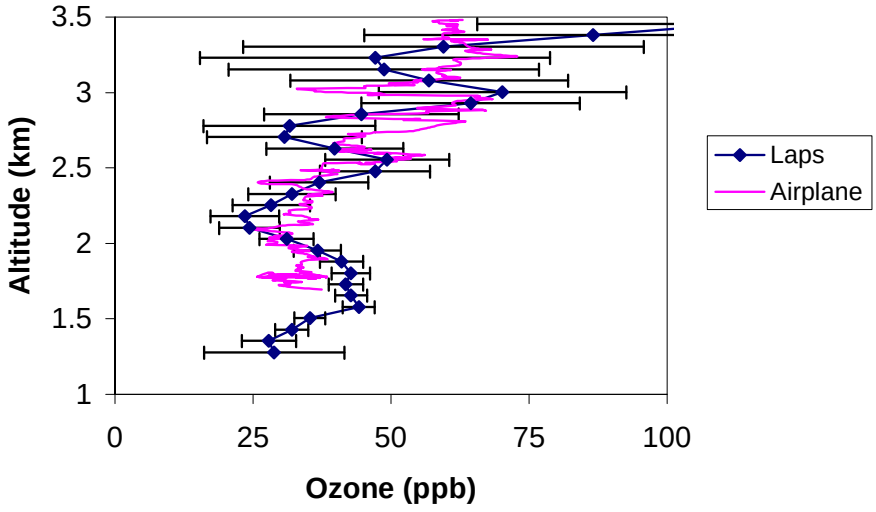

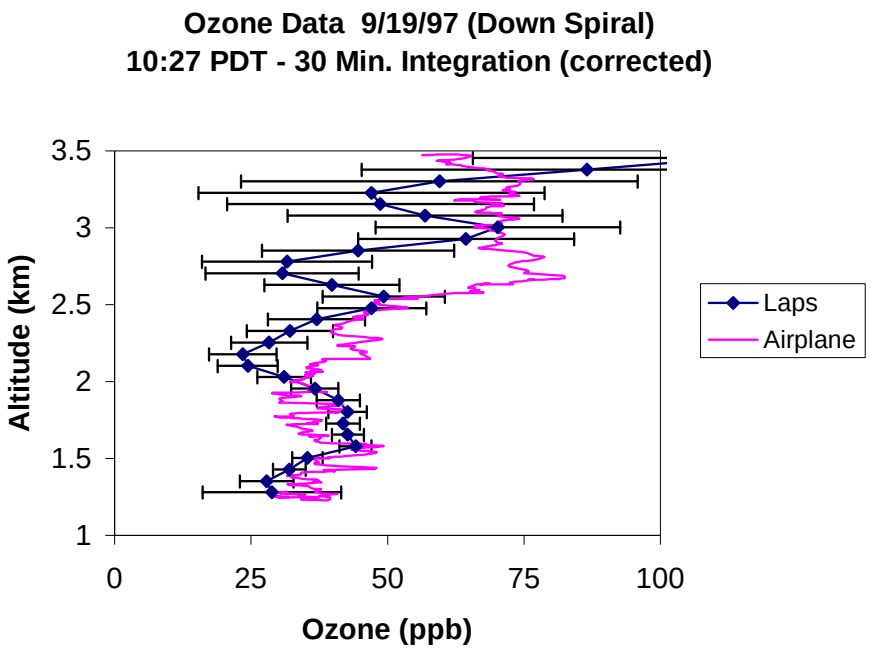
Ozone Data 9/19/97 (Down Spiral)
10:27 PDT - 30 Min. Integration (corrected)
Altitude (km)
3.5
3
2.5
2
1.5
1
0
25
50
75
100
Ozone (ppb)
Laps
Airplane

Water Vapor Data

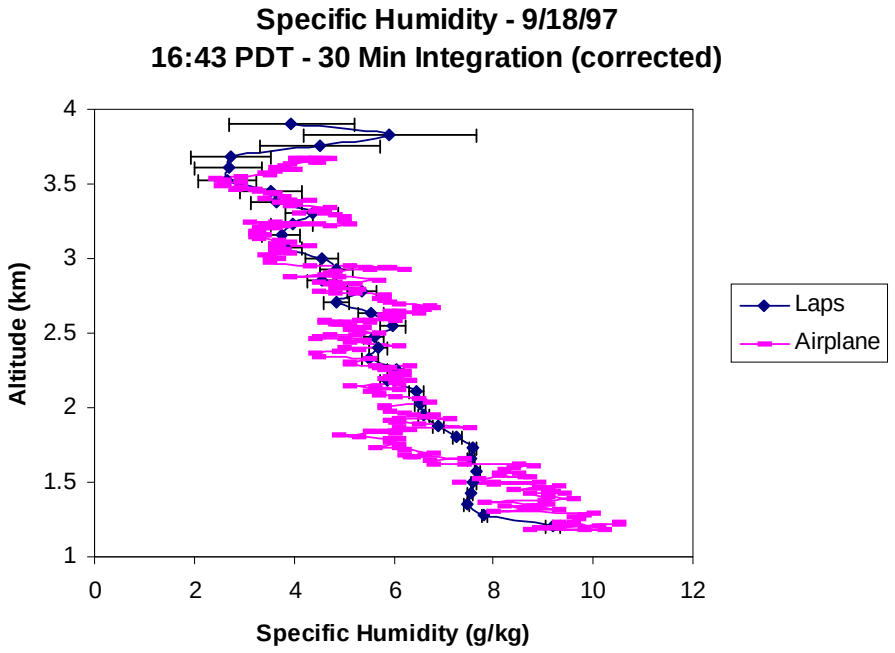

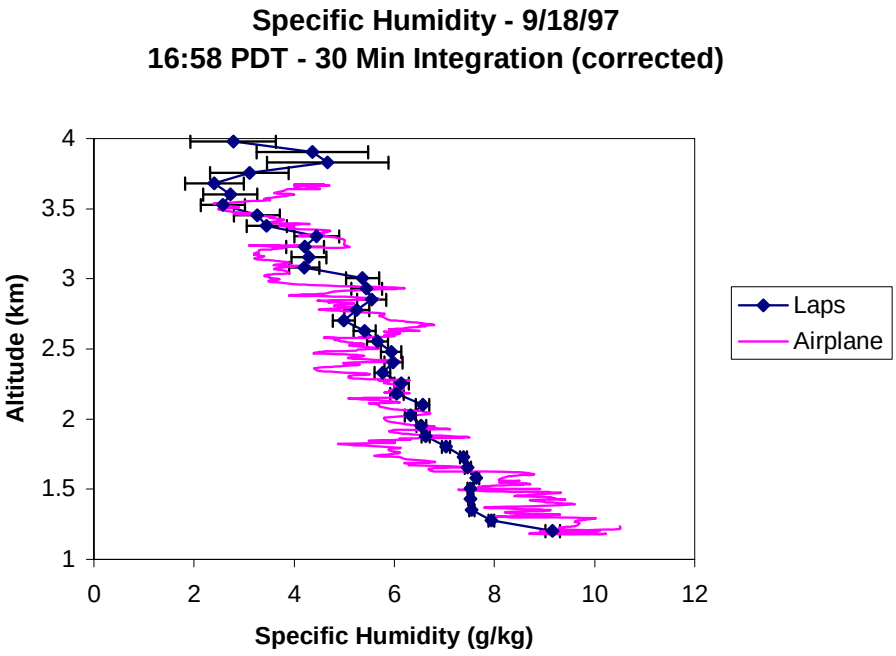

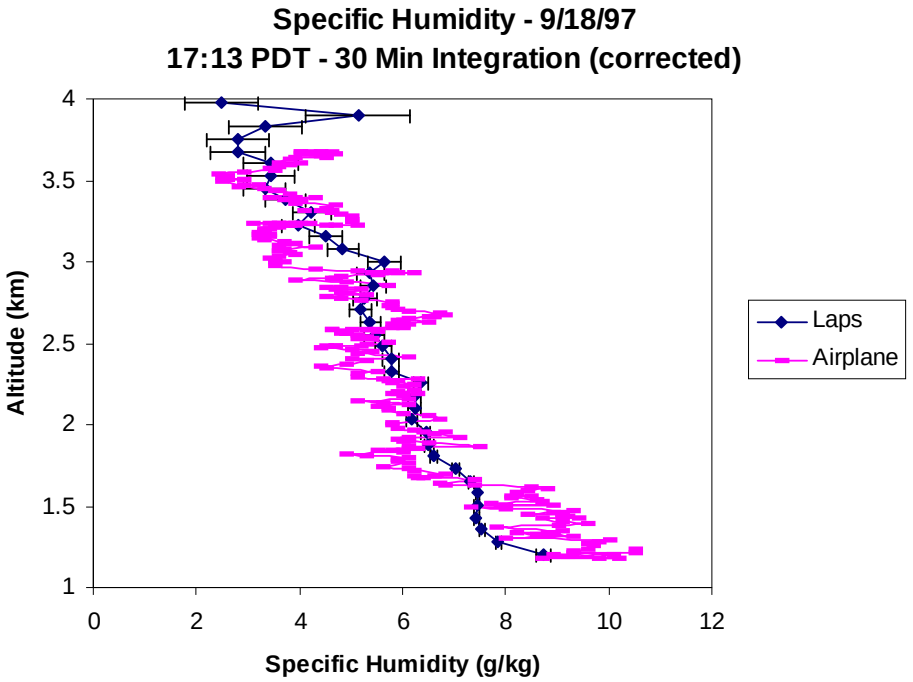
Specific Humidity - 9/18/97
17:13 PDT - 30 Min Integration (corrected)
Altitude (km)
4
3.5
3
2.5
2
1.5
1
0
2
4
6
8
10
12
Specific Humidity (g/kg)
Laps
Airplane

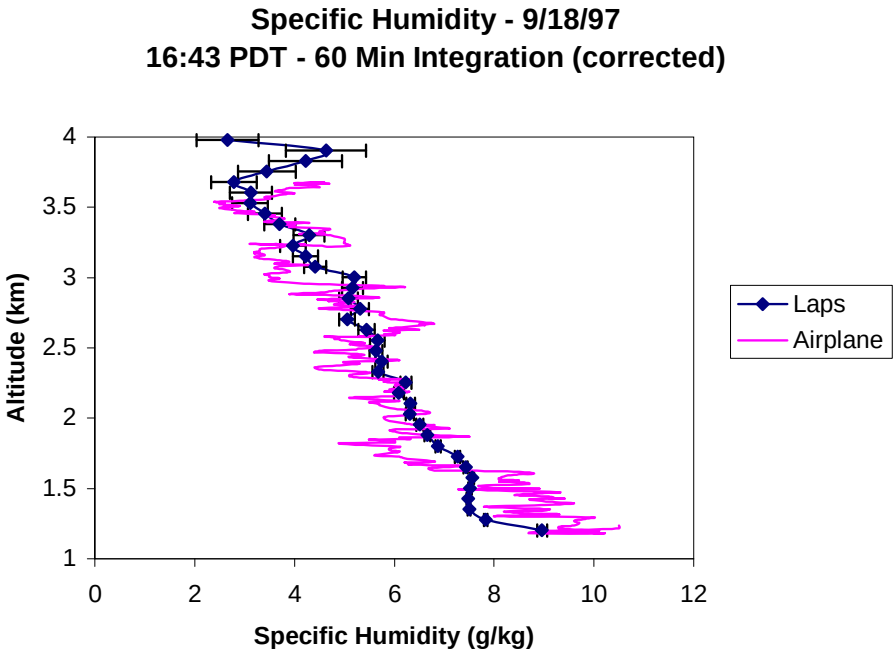
Specific Humidity - 9/18/97
16:43 PDT - 60 Min Integration (corrected)
Altitude (km)
4
3.5
3
2.5
2
1.5
1
0
2
4
6
8
10
12
Specific Humidity (g/kg)
Laps
Airplane

Specific Humidity - 9/18/97 (Up Spiral)
20:35 PDT - 30 Min Integration (corrected)

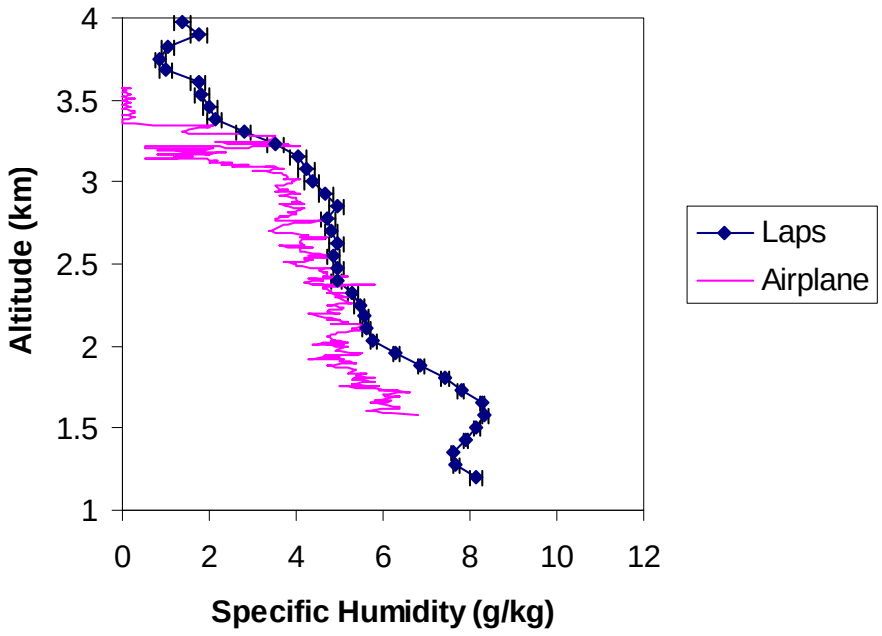

Specific Humidity - 9/18/97 (Up Spiral)
21:06 PDT - 30 Min Integration (corrected)

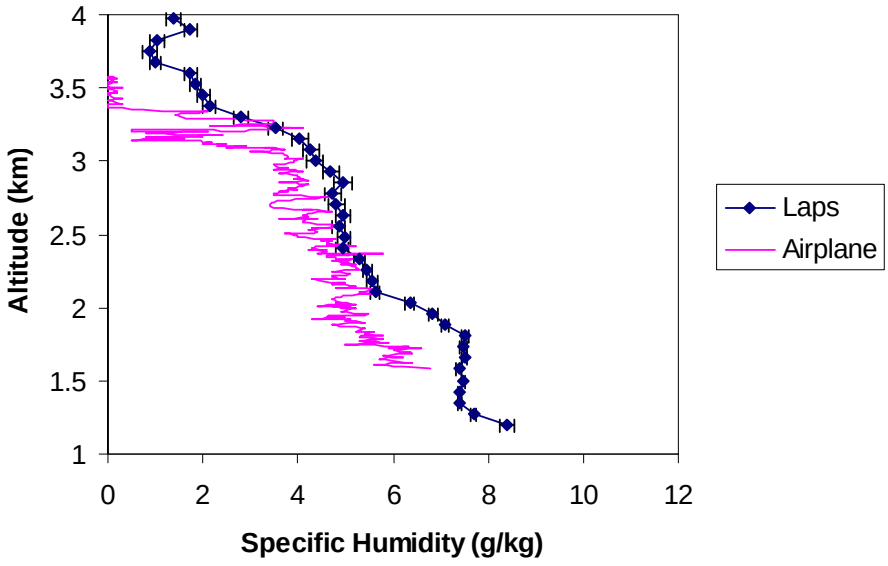

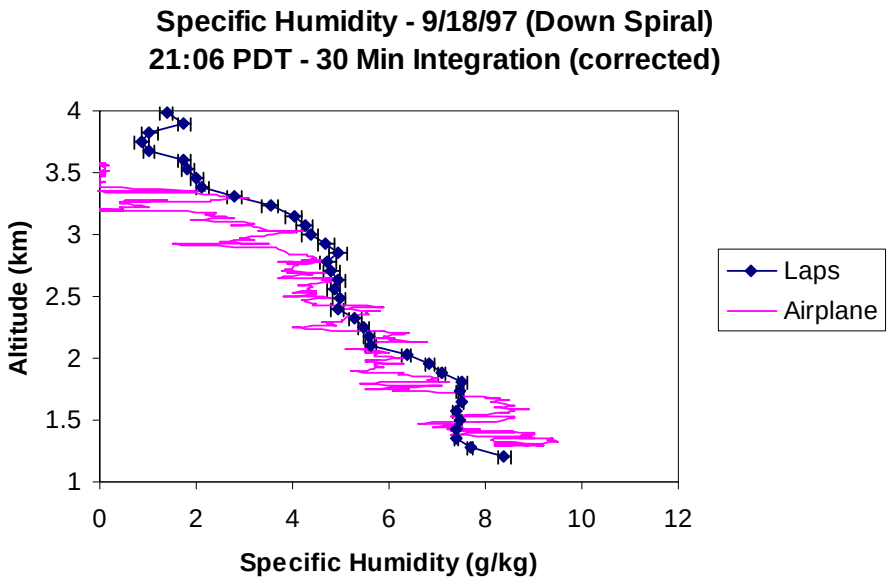
Specific Humidity - 9/18/97 (Down Spiral)
21:06 PDT - 30 Min Integration (corrected)
Altitude (km)
4
3.5
3
2.5
2
1.5
1
0
2
4
6
8
10
12
Specific Humidity (g/kg)
Laps
Airplane

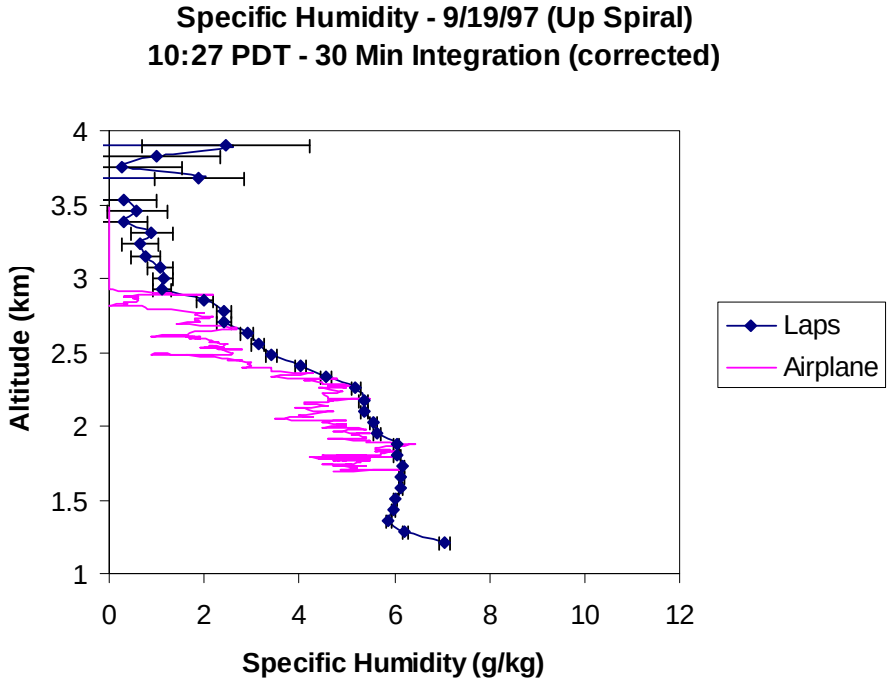
Specific Humidity - 9/19/97 (Up Spiral)
10:27 PDT - 30 Min Integration (corrected)
Altitude (km)
4
3.5
3
2.5
2
1.5
1
0
2
4
6
8
10
12
Specific Humidity (g/kg)
Laps
Airplane

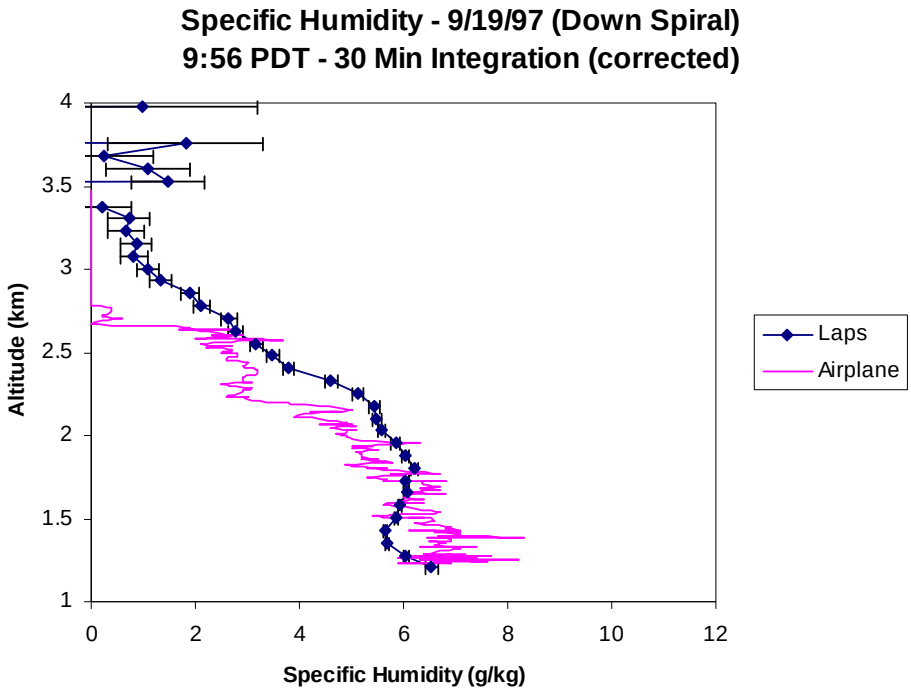
Specific Humidity - 9/19/97 (Down Spiral)
9:56 PDT - 30 Min Integration (corrected)
Altitude (km)
4
3.5
3
2.5
2
1.5
1
0
2
4
6
8
10
12
Specific Humidity (g/kg)
Laps
Airplane

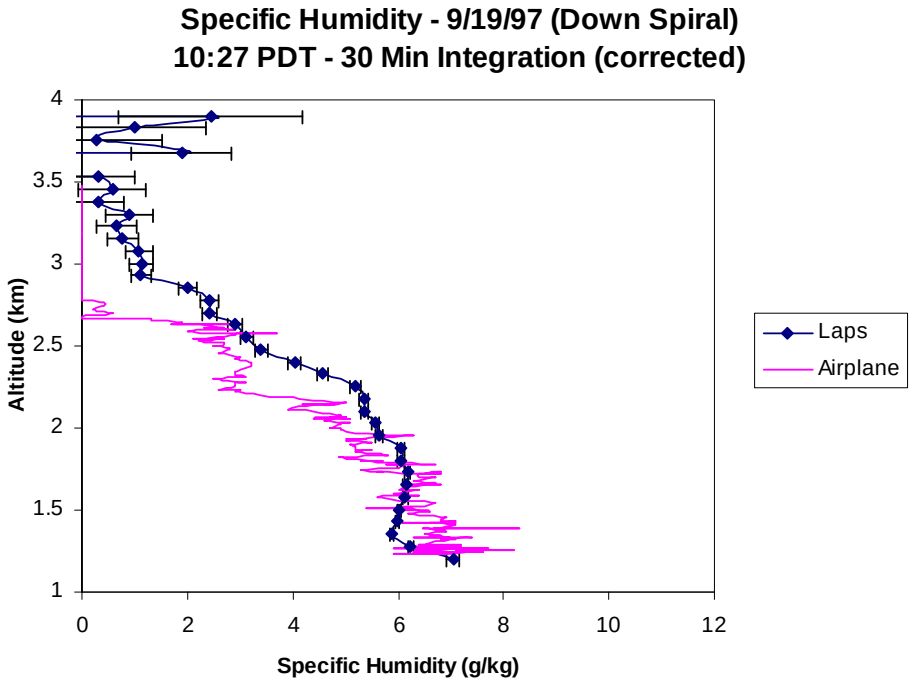
Specific Humidity - 9/19/97 (Down Spiral)
10:27 PDT - 30 Min Integration (corrected)
Altitude (km)
4
3.5
3
2.5
2
1.5
1
0
2
4
6
8
10
12
Specific Humidity (g/kg)
Laps
Airplane

Appendix B

Data Processing Programs

This section contains matlab source code used to make the time sequence color plots. The functions ozone and water bring up graphical user interface windows that make it easy to obtain a data output. These functions call tsozone and tswat respectively.

```
function ozone()
% This is the machine-generated representation of a Handle Graphics object
% and its children.  Note that handle values may change when these objects
% are re-created. This may cause problems with any callbacks written to
% depend on the value of the handle at the time the object was saved.
%
% To reopen this object, just type the name of the M-file at the MATLAB
% prompt. The M-file and its associated MAT-file must be on your path.

load ozone

a = figure('Color',[0.8 0.8 0.8], ...
      'Colormap',mat0, ...
      'PointerShapeCData',mat1, ...
      'Position',[234 148 560 390], ...
      'Tag','popupmenu1');
b = uicontrol('Parent',a, ...
      'Units','points', ...
      'BackgroundColor',[0 1 1], ...
      'Position',[47.25 225 101.25 23.25], ...
      'String','Enter maximum contour value in ppb', ...
      'Style','text', ...
      'Tag','StaticText1');
b = uicontrol('Parent',a, ...
      'Units','points', ...
      'BackgroundColor',[0 1 1], ...
      'Position',[327.75 231 82.5 18], ...
      'String','Enter Maximum Altitude (meters)', ...
      'Style','text', ...
      'Tag','StaticText1');
b = uicontrol('Parent',a, ...
      'Units','points', ...
      'BackgroundColor',[0 1 1], ...
      'Position',[172.5 229.5 130.5 18], ...
      'String','Enter: (integration time)/2  if integer or  (integration time)/2 -1', ...
      'Style','text', ...
      'Tag','StaticText1');
b = uicontrol('Parent',a, ...
      'Units','points', ...
      'BackgroundColor',[0 1 1], ...
      'Position',[44.25 179.25 82.5 18], ...
      'String','Enter the step size (min)l', ...
      'Style','text', ...
```

```
        'Tag','StaticText1');
    b = uicontrol('Parent',a, ...
        'Units','points', ...
        'BackgroundColor',[1 1 1], ...
        'Position',[48 201.75 99.75 21.75], ...
        'String','100', ...
        'Style','edit', ...
        'Tag','maxval');
    b = uicontrol('Parent',a, ...
        'Units','points', ...
        'BackgroundColor',[1 1 1], ...
        'Position',[173.25 204 130.5 24.75], ...
        'String','15', ...
        'Style','edit', ...
        'Tag','int');
    b = uicontrol('Parent',a, ...
        'Units','points', ...
        'BackgroundColor',[1 1 1], ...
        'Position',[327.75 208.5 81.75 21.75], ...
        'String','3500', ...
        'Style','edit', ...
        'Tag','maxalt');
    b = uicontrol('Parent',a, ...
        'Units','points', ...
        'BackgroundColor',[1 1 1], ...
        'Position',[45 156 83.25 21.75], ...
        'String','5', ...
        'Style','edit', ...
        'Tag','step');
    b = uicontrol('Parent',a, ...
        'Units','points', ...
        'Callback','tsozone', ...
        'Position',[267 30.75 100.5 29.25], ...
        'String','Make O3 plot', ...
        'Tag','Pushbutton1');
    b = uicontrol('Parent',a, ...
        'Units','points', ...
        'BackgroundColor',[0 1 1], ...
        'Position',[49.5 28.5 162 32.25], ...
        'String','Check if Processing Alaska March data', ...
        'Style','checkbox', ...
        'Tag','unit');
    b = uicontrol('Parent',a, ...
        'Units','points', ...
        'BackgroundColor',[0 1 1], ...
        'FontSize',14, ...
        'FontWeight','bold', ...
        'Position',[129.75 260.25 195.75 23.25], ...
        'String','Time Sequence Of Ozone', ...
        'Style','text', ...
        'Tag','StaticText2');
    b = uicontrol('Parent',a, ...
        'Units','points', ...
        'BackgroundColor',[1 1 1], ...
        'Position',[168 154.5 100.5 24.75], ...
```

```
        'String',['1997';'1996';'1998';'1999'], ...
        'Style','popupmenu', ...
        'Tag','year', ...
        'Value',1);
    b = uicontrol('Parent',a, ...
        'Units','points', ...
        'BackgroundColor',[0 1 1], ...
        'Position',[167.25 180.75 100.5 12], ...
        'String','Select Year', ...
        'Style','text', ...
        'Tag','StaticText3');
    b = uicontrol('Parent',a, ...
        'Units','points', ...
        'BackgroundColor',[0 1 1], ...
        'Position',[288.75 180 100.5 13.5], ...
        'String','Select Time Zone', ...
        'Style','text', ...
        'Tag','StaticText3');
    b = uicontrol('Parent',a, ...
        'Units','points', ...
        'BackgroundColor',[1 1 1], ...
        'Position',[288.75 153.75 100.5 24.75], ...
        'String',['PDT';'AST';'UTC';'PST';'EDT';'EST'], ...
        'Style','popupmenu', ...
        'Tag','TZ', ...
        'Value',1);
    b = uicontrol('Parent',a, ...
        'Units','points', ...
        'BackgroundColor',[1 1 1], ...
        'Position',[44.25 83.25 83.25 21.75], ...
        'String','.5', ...
        'Style','edit', ...
        'Tag','sig_clip');
    b = uicontrol('Parent',a, ...
        'Units','points', ...
        'BackgroundColor',[0 1 1], ...
        'Position',[40.5 105 99 12.75], ...
        'String','Input c', ...
        'Style','text', ...
        'Tag','StaticText1');
    b = uicontrol('Parent',a, ...
        'Units','points', ...
        'BackgroundColor',[0 1 1], ...
        'Position',[40.5 117 98.25 19.5], ...
        'String',' Enter clipping variable      i.e. clip at   std > c * water', ...
        'Style','text', ...
        'Tag','StaticText1');
    b = uicontrol('Parent',a, ...
        'Units','points', ...
        'BackgroundColor',[0 1 1], ...
        'Position',[41.25 117.75 98.25 19.5], ...
        'String',' Enter clipping variable      i.e. clip at   std > c * ozone', ...
        'Style','text', ...
        'Tag','StaticText1');
```

```
%-------------------------------------------------------
%  Program:       Reads and outputs Ozone Data
%  Programmed By: Steve Esposito
%
%   Program changed on 09\13\98 - Steven Esposito
%   Changes for clipping the data at the top of the plot.
%   This file reads the data from the files from the LAPS_DSP
%   program and outputs three arrays containing the altitude,
%   signal and error.  Use program in conjunction with tsO3clip.m
%
%
%   changed 09/18/98 to pick off name from file list
%
%   Changed 10/6/98 to accomodate for gui inputs - run ozone.m first for
%  graphic user interface
%
%   Changed 12/10/98 to leave white spaces where data does not exist
%
%-------------------------------------------------------


function tsozone
%  Time sequence Ozone data program accepting files from Laps_Dsp
%   program.

% Getting the inputs from the Graphical user interface screen

HH = findobj(gcf,'Tag','maxval');
maxval = str2num(get(HH,'String'));

HH = findobj(gcf,'Tag','maxalt');
maxalt = str2num(get(HH,'String'));

HH = findobj(gcf,'Tag','int');
int = str2num(get(HH,'String'));

HH = findobj(gcf,'Tag','step');
step = str2num(get(HH,'String'));

HH = findobj(gcf,'Tag','unit');
unit = (get(HH,'value'));

HH = findobj(gcf,'Tag','year');
year = (get(HH,'value'));

HH = findobj(gcf,'Tag','sig_clip');
sig_clip = str2num(get(HH,'String'));



%   Taking the value from the GUI screen and changing it into a string
%   containing the year

switch year
case 1
```

```
  year=num2str(97);
case 2
  year=num2str(96);
case 3
  year=num2str(98);
case 4
  year=num2str(99);
end



%   Taking the value from the GUI screen and changing it into a string
%   containing the time zone

HH = findobj(gcf,'Tag','TZ');
TZ = (get(HH,'value'));

switch TZ
case 1
  TZ=['PDT'];
case 2
  TZ=['AST'];
case 3
  TZ=['UTC'];
case 4
  TZ=['PST'];
case 5
  TZ=['EDT'];
case 6
  TZ=['EST'];
end

save_loc=cd;  %  Save what directory the matlab mfiles are running in

%   Pick any file from the directory where the data is stored
[fi,pa]=uigetfile('h:\scos\scosnew\scos30\*.dat','Please select any file in the directory to be processed');


%   Change pointer to hour glass

setptr(1,'watch');

%   Change directory to where the files are located, make a list of all the files,
%   and load that list into Matlab as a vector

cd (pa);
!dir /b *.dat >list.txt
load list.txt;

filename=sort(list);     %   Sort the List so the minutes are in ascending order

%   If fifteen or more consecutive minutes are missing plot a white space
%   This does not take into account missing whole days of data
%
%   The ith element of var_step contains the number N
```

```
%    N is the number of missing minutes until the next minute


for i=1:(length(filename)-1)
  tempmin=filename(1:length(filename));
  mincheckaa=num2str(tempmin(i+1));
  mincheckbb=num2str(tempmin(i));
  minchecka=str2num(mincheckaa((length(mincheckaa)-1):length(mincheckaa)));
  mincheckb=str2num(mincheckbb((length(mincheckbb)-1):length(mincheckbb)));
  hourchecka=str2num(mincheckaa((length(mincheckaa)-3):length(mincheckaa)-2));
  hourcheckb=str2num(mincheckbb((length(mincheckbb)-3):length(mincheckbb)-2));

  if( minchecka - mincheckb < 0)
    var_step(i+1)=tempmin(i+1) - tempmin(i) - step -40;
  else
     var_step(i+1)=tempmin(i+1) - tempmin(i) - step;
  end
  if hourchecka - hourcheckb < 0
    var_step(i+1)=var_step(i+1)-7600;
  end
end



for i=1:length(var_step)
 if (var_step(i) <= 15)
   var_step(i)=0;
 end
end


%    Variables to be set if there is a problem with the header

bitsetstart=0;
bitsetend=0;
startmin=['**'];
endmin=['**'];

if unit ==1
  cd (save_loc);
  [a,b]=utcfix(filename(1),filename(length(filename)));
  cd(pa);
else
  a=num2str(filename(1));
  b=num2str(filename(length(filename)));
end


%    Change back to the directory where mfiles are located

cd (save_loc);

%    Call subroutine to make header.  Output of timehead
%    is the date information for the title of the plot then
%    make a vector with the plot title in it
```

```
header=timehead(a,b,int,year);
name=['Time Sequence Of Ozone - ' header ' ' TZ];

%   Change back to the directory where the data files are located

cd(pa);

%   Open data files and peel out necessary information for the plot
%   (Altitude, Ozone Density ( ppb ) and Standard deviation
%   of composite Ozone Densigy measurement ( ppb )

if length(a)==7
  for i = 1:length(filename)
        path=['\0' num2str(filename(i)) '.dat'];
        fid = fopen(path, 'r');
    fscanf(fid, '%255char');
        Da =    fscanf(fid, '%f', [17, inf]);
    fclose(fid);
    Alt(:,i)=Da(1,:)';
    O3(:,i)=Da(10, :)';
    stdO3(:,i)=Da(11,:)';
  end
else
  for i = 1:length(filename)
        path=[num2str(filename(i)) '.dat'];
        fid = fopen(path, 'r');
    fscanf(fid, '%255char');
        Da =    fscanf(fid, '%f', [17, inf]);
    fclose(fid);
    Alt(:,i)=Da(1,:)';
    O3(:,i)=Da(10, :)';
    stdO3(:,i)=Da(11,:)';
  end
end

clear Da;

%   Clip the measurements to values below the maximum altitude
%   specified by user

ind=find(Alt(:,1) > 0 & Alt(:,1)< maxalt);
Alt=Alt(ind,:);
O3=O3(ind,:);
stdO3=stdO3(ind,:);

a=size(O3);

%   Change the -99 values in the columns of the array to the value in
%   the previous row, or if it the first row, change it to the first
%   number not equal to -99.


for j=1:a(2)
  for i=1:a(1)
```

```
            if (O3(i,j)==-99 & i == 1)
        ind=find(O3(:,j) ~= -99);
        O3(i,j)=O3(min(ind),j);
        stdO3(i,j)=stdO3(min(ind),j);
        clear ind;
            end
            if (O3(i,j)==-99 & i ~= 1)
            O3(i,j)=O3(i-1,j);
            stdO3(i,j)=1;
            end
    end
  end


%    If the signal is higher than 200 clip it to 200

  for j=1:a(2)
   for i=1:a(1)
     if (O3(i,j) > 200)
       O3(i,j) = 200;
            stdO3(i,j)=1;
     end
   end
end



%    Make an array with columns of zeros for missing minutes

O3a=zeros(a(1),(length(var_step)+sum(var_step)));
stdO3a=zeros(a(1),(length(var_step)+sum(var_step)));

i=1;
for j=1:(length(var_step))
  if var_step(j)==0
     O3a(:,i)=O3(:,j);
     stdO3a(:,i)=stdO3(:,j);
     alta(:,i)=Alt(:,j);
  else
     i=i+var_step(j)/step;
     O3a(:,i)=O3(:,j);
     stdO3a(:,i)=stdO3(:,j);
     alta(:,i)=Alt(:,j);
end

i=i+1;
end

O3=O3a;
Alt=alta;
stdO3=stdO3a;
Alt=Alt./1000;
a=size(Alt);
figure;
```

```
%    Check for columns of zeros.  If a column of zeros exists plot a white space
%    Check that the std of the measuremant is not > a * signal (a is a constant
%    inputted from the GUI screen.  If it is clip at the top.

for j=1:a(2)-1;
  for i=5:a(1)
          if (O3(:,j) == 0 | O3(:,j+1)==0 & (stdO3(:,j)==0 | stdO3(:,j+1)==0))
    break ; end;
     if ((stdO3(i,j) > sig_clip*O3(i,j)) | (stdO3(i,j+1) > sig_clip*O3(i,j+1) | i==a(1)));
       pcolor([j j+1],[Alt(1:(i-1),j) Alt(1:(i-1),j)],...
       [O3(1:(i-1),j) O3(1:(i-1),j+1)]);
      hold on;
       break; end;
      end
end

%    Plot labeling information
axis([1 a(2) Alt(1,1) Alt(a(1),1)])
shading interp;
h1=get(gca,'clim');
set(gca,'clim',[h1(1) maxval]);
barhan=colorbar('horiz');
axhan=gca;

h=title(name);
set(h,'fontname','timesnewroman','fontsize',14)
h=xlabel('Time (minutes)');
set(h,'fontname','timesnewroman','fontsize',12)
h=ylabel('Altitude (km)');
set(h,'fontname','timesnewroman','fontsize',12)
axes(barhan);
h=xlabel('Ozone (PPB)');
set(h,'fontname','timesnewroman','fontsize',12)
axes(axhan);


%    Set the x axis label to the correct step size
if step ~=1
      h=get(gca,'xticklabel');
      set(gca,'xticklabel',num2str(step.*str2num(h)));
end

%    Change back to directory where mfiles are located and
%    set pointer to arrow.

cd (save_loc);
setptr(1,'arrow');


%    For error in header
if (bitsetstart==1 & bitsetend==1)
  stringinput=('Both the beginning and ending minute - the integration time is < 0 ...  Please delete bad files
or enter title manually');
  bitsetstart=0; bitsetend=0;
```

```
  reply=warndlg(stringinput,'WARNING');
end

if (bitsetstart==1)
  stringinput=('The beginning minute - the integration time is < 0 ...  Please delete bad files or enter title
manually');
  reply=warndlg(stringinput,'WARNING');
end

if (bitsetend==1)
     stringinput=('The ending minute - the integration time is < 0...  Please delete bad files or enter title
manually');
  reply=warndlg(stringinput,'WARNING');
end



function water()
% This is the machine-generated representation of a Handle Graphics object
% and its children.  Note that handle values may change when these objects
% are re-created. This may cause problems with any callbacks written to
% depend on the value of the handle at the time the object was saved.
%
% To reopen this object, just type the name of the M-file at the MATLAB
% prompt. The M-file and its associated MAT-file must be on your path.

load water

a = figure('Color',[0.8 0.8 0.8], ...
      'Colormap',mat0, ...
      'PointerShapeCData',mat1, ...
      'Position',[149 184 560 390], ...
      'Tag','popupmenu1');
b = uicontrol('Parent',a, ...
      'Units','points', ...
      'BackgroundColor',[0 1 1], ...
      'Position',[42 232.5 101.25 23.25], ...
      'String','Enter maximum contour value g/kg', ...
      'Style','text', ...
      'Tag','StaticText1');
b = uicontrol('Parent',a, ...
      'Units','points', ...
      'BackgroundColor',[0 1 1], ...
      'Position',[326.25 234 82.5 18], ...
      'String','Enter Maximum Altitude (meters)', ...
      'Style','text', ...
      'Tag','StaticText1');
b = uicontrol('Parent',a, ...
      'Units','points', ...
      'BackgroundColor',[0 1 1], ...
      'Position',[168 234 130.5 18], ...
      'String','Enter: (integration time)/2  if integer or  (integration time)/2 -1', ...
      'Style','text', ...
      'Tag','StaticText1');
b = uicontrol('Parent',a, ...
```

```
        'Units','points', ...
        'BackgroundColor',[0 1 1], ...
        'Position',[42 174 82.5 19.5], ...
        'String','Enter the step size (min)l', ...
        'Style','text', ...
        'Tag','StaticText1');
    b = uicontrol('Parent',a, ...
        'Units','points', ...
        'BackgroundColor',[1 1 1], ...
        'Position',[42 208.5 99.75 23.25], ...
        'String','10', ...
        'Style','edit', ...
        'Tag','maxval');
    b = uicontrol('Parent',a, ...
        'Units','points', ...
        'BackgroundColor',[1 1 1], ...
        'Position',[168 216.75 130.5 16.5], ...
        'String','2', ...
        'Style','edit', ...
        'Tag','int');
    b = uicontrol('Parent',a, ...
        'Units','points', ...
        'BackgroundColor',[1 1 1], ...
        'Position',[326.25 212.25 83.25 21.75], ...
        'String','3500', ...
        'Style','edit', ...
        'Tag','maxalt');
    b = uicontrol('Parent',a, ...
        'Units','points', ...
        'BackgroundColor',[1 1 1], ...
        'Position',[42 152.25 82.5 21.75], ...
        'String','1', ...
        'Style','edit', ...
        'Tag','step');
    b = uicontrol('Parent',a, ...
        'Units','points', ...
        'Callback','tswat', ...
        'Position',[252 31.5 100.5 29.25], ...
        'String','Make WV plot', ...
        'Tag','Pushbutton1');
    b = uicontrol('Parent',a, ...
        'Units','points', ...
        'BackgroundColor',[0 1 1], ...
        'Position',[42.75 30 162 32.25], ...
        'String','Check if Processing Alaska March data', ...
        'Style','checkbox', ...
        'Tag','unit');
    b = uicontrol('Parent',a, ...
        'Units','points', ...
        'BackgroundColor',[0 1 1], ...
        'FontSize',14, ...
        'FontWeight','bold', ...
        'Position',[44.25 267 347.25 23.25], ...
        'String','Time Sequence Water Vapor Processing', ...
        'Style','text', ...
```

```
        'Tag','StaticText2');
    b = uicontrol('Parent',a, ...
        'Units','points', ...
        'BackgroundColor',[1 1 1], ...
        'Position',[168 149.25 100.5 24.75], ...
        'String',['1997';'1996';'1998';'1999'], ...
        'Style','popupmenu', ...
        'Tag','year', ...
        'Value',3);
    b = uicontrol('Parent',a, ...
        'Units','points', ...
        'BackgroundColor',[0 1 1], ...
        'Position',[168 174.75 100.5 12], ...
        'String','Select Year', ...
        'Style','text', ...
        'Tag','StaticText3');
    b = uicontrol('Parent',a, ...
        'Units','points', ...
        'BackgroundColor',[0 1 1], ...
        'Position',[293.25 174.75 100.5 13.5], ...
        'String','Select Time Zone', ...
        'Style','text', ...
        'Tag','StaticText3');
    b = uicontrol('Parent',a, ...
        'Units','points', ...
        'BackgroundColor',[1 1 1], ...
        'Position',[293.25 150 100.5 24.75], ...
        'String',['PDT';'AST';'UTC';'PST';'EDT';'EST'], ...
        'Style','popupmenu', ...
        'Tag','TZ', ...
        'Value',1);
    b = uicontrol('Parent',a, ...
        'Units','points', ...
        'BackgroundColor',[1 1 1], ...
        'Position',[42 85.5 99.75 21.75], ...
        'String','0.2', ...
        'Style','edit', ...
        'Tag','sig_clip');
    b = uicontrol('Parent',a, ...
        'Units','points', ...
        'BackgroundColor',[0 1 1], ...
        'Position',[42 116.25 99 19.5], ...
        'String',' Enter clipping variable       i.e. clip at   std > c * water', ...
        'Style','text', ...
        'Tag','StaticText1');
    b = uicontrol('Parent',a, ...
        'Units','points', ...
        'BackgroundColor',[0 1 1], ...
        'Position',[42 106.5 99.75 11.25], ...
        'String','Input c', ...
        'Style','text', ...
        'Tag','StaticText1');
    b = uicontrol('Parent',a, ...
        'Units','points', ...
        'BackgroundColor',[0 1 1], ...
```

```
'Position',[168.75 116.25 69.75 18.75], ...
'String','Smoothing On', ...
'Style','radiobutton', ...
'Tag','smooth');
```

```
%-----------------------------------------------------------
%  Program:       Reads and outputs WV Data
%  Programmed By: Steve Esposito
%
%    Program changed on 09\13\98 - Steven Esposito
%    Changes for clipping the data at the top of the plot.
%    This file reads the data from the files from the LAPS_DSP
%    program and outputs three arrays containing the altitude,
%    signal and error.  Use program in conjunction with tswatclip.m
%
%
%    changed 09/18/98 to pick off name from file list
%
%    Changed 10/6/98 to accomodate for gui inputs - run water.m first for
%  graphic user interface
%-----------------------------------------------------------


function tswat
%  Time sequence UV water vapor data program accepting files from Laps_Dsp
%    program.
clear all;

% Getting the inputs from the Graphical user interface screen

HH = findobj(gcf,'Tag','maxval');
maxval = str2num(get(HH,'String'));

HH = findobj(gcf,'Tag','maxalt');
maxalt = str2num(get(HH,'String'));

HH = findobj(gcf,'Tag','int');
int = str2num(get(HH,'String'));

HH = findobj(gcf,'Tag','step');
step = str2num(get(HH,'String'));

HH = findobj(gcf,'Tag','sig_clip');
sig_clip = str2num(get(HH,'String'));

HH = findobj(gcf,'Tag','unit');
unit = (get(HH,'value'));

HH = findobj(gcf,'Tag','year');
year = (get(HH,'value'));

HH = findobj(gcf,'Tag','smooth');
smooth = (get(HH,'value'));


%    Taking the value from the GUI screen and changing it into a string
%    containing the year

switch year
case 1
```

```
  year=num2str(97);
case 2
  year=num2str(96);
case 3
  year=num2str(98);
case 4
  year=num2str(99);
end

HH = findobj(gcf,'Tag','TZ');
TZ = (get(HH,'value'));

%   Taking the value from the GUI screen and changing it into a string
%   containing the time zone

switch TZ
case 1
  TZ=['PDT'];
case 2
  TZ=['AST'];
case 3
  TZ=['UTC'];
case 4
  TZ=['PST'];
case 5
  TZ=['EDT'];
case 6
  TZ=['EST'];
end

save_loc=cd;%   Save what directory the matlab mfiles are running in

%   Pick any file from the directory where the data is stored

[fi,pa]=uigetfile('h:\scos\scosnew\scos5\*.dat','Please select any file in the directory to be processed');

%   Change pointer to hour glass

setptr(1,'watch');

%   Change directory to where the files are located, make a list of all the files,
%   and load that list into Matlab as a vector

cd (pa);
!dir /b *.dat >list.txt
load list.txt;

filename=sort(list);          %   Sort the List so the minutes are in ascending order

%   If five or more consecutive minutes are missing plot a white space
%   This does not take into account missing whole days of data
%
%   The ith element of var_step contains the number N
%   N is the number of missing minutes until the next minute
```

```
for i=1:(length(filename)-1)
  tempmin=filename(1:length(filename));
  mincheckaa=num2str(tempmin(i+1));
  mincheckbb=num2str(tempmin(i));
  minchecka=str2num(mincheckaa((length(mincheckaa)-1):length(mincheckaa)));
  mincheckb=str2num(mincheckbb((length(mincheckbb)-1):length(mincheckbb)));
  hourchecka=str2num(mincheckaa((length(mincheckaa)-3):length(mincheckaa)-2));
  hourcheckb=str2num(mincheckbb((length(mincheckbb)-3):length(mincheckbb)-2));

  if( minchecka - mincheckb < 0)
    var_step(i+1)=tempmin(i+1) - tempmin(i) - step -40;
  else
     var_step(i+1)=tempmin(i+1) - tempmin(i) - step;
  end
  if hourchecka - hourcheckb < 0
    var_step(i+1)=var_step(i+1)-7600;
  end
end



for i=1:length(var_step)
 if (var_step(i) <= 5)
   var_step(i)=0;
 end
end


%   Variables to be set if there is a problem with the header

bitsetstart=0;
bitsetend=0;
startmin=['**'];
endmin=['**'];

%   Changes the times to UTC for the Alaska March data

if unit ==1
  cd (save_loc);
  [a,b]=utcfix(filename(1),filename(length(filename)));
  cd(pa);
else
  a=num2str(filename(1));
  b=num2str(filename(length(filename)));
end

%   Change back to the directory where mfiles are located

cd (save_loc);

%   Call subroutine to make header.  Output of timehead
%   is the date information for the title of the plot then
%   make a vector with the plot title in it

header=timehead(a,b,int,year);
```

```
name=['Water Vapor Mixing Ratio - ' header ' ' TZ];

%   Change back to the directory where the data files are located

cd(pa);

%   Open data files and peel out necessary information for the plot
%   (Altitude, Composite water vapor ( g / kg ) and Standard deviation
%   of composite water vapor maesurement ( g / kg )

if length(a)==7
  for i = 1:length(filename)
          path=['\0' num2str(filename(i)) '.dat'];
          fid = fopen(path, 'r');
     fscanf(fid, '%255char');
          Da =     fscanf(fid, '%f', [17, inf]);
     fclose(fid);
    Alt(:,i)=Da(1,:)';
     wat(:,i)=Da(2, :)';
     stdwat(:,i)=Da(3,:)';
  end
else
  for i = 1:length(filename)
          path=[num2str(filename(i)) '.dat'];
          fid = fopen(path, 'r');
     fscanf(fid, '%255char');
          Da =     fscanf(fid, '%f', [17, inf]);
     fclose(fid);
     Alt(:,i)=Da(1,:)';
     wat(:,i)=Da(2, :)';
     stdwat(:,i)=Da(3,:)';
  end
end

clear Da;

%   Clip the measurements to values below the maximum altitude

ind=find(Alt(:,1) > 0 & Alt(:,1)< maxalt);
Alt=Alt(ind,:);
wat=wat(ind,:);
stdwat=stdwat(ind,:);

a=size(wat);

%   Change the -99 values in the columns of the array to 0 if it is in
%   the first row or to the value in the previous row if it is in a row
%   greater than the first row

for j=1:a(2)
  for i=1:a(1)
          if (wat(i,j)==-99 & i == 1)
       wat(i,j)=0.001;
       stdwat(i,j)=0.001;
          end
```

```
            if (wat(i,j)==-99 & i ~= 1)
            wat(i,j)=wat(i-1,j);
            stdwat(i,j)=std(i-1,j);
            end
    end
  end

%    If the signal is higher than 20 clip it to 20

for j=1:a(2)
   for i=1:a(1)
      if (wat(i,j) > 20)
         wat(i,j) = 20;
    %       stdwat(i,j)=1000;
      end
   end
end

b=1;
%smoothing
if smooth==1;
b=11;
clear a;
a=size(Alt)
for j=11:(a(2)-11)
        for i=3:(a(1)-3)
        signal_matb=[wat(i-2,j-10) wat(i-1,j-10) wat(i,j-10) wat(i+1,j-10) wat(i+2,j-10)...
                wat(i-2,j-5) wat(i-1,j-5)wat(i,j-5) wat(i+1,j-5) wat(i+2,j-5)...
                wat(i-2,j) wat(i-1,j)wat(i,j) wat(i+1,j) wat(i+2,j)...
                wat(i-2,j+5) wat(i-1,j+5)wat(i,j+5) wat(i+1,j+5) wat(i+2,j+5)...
                   wat(i-2,j+10) wat(i-1,j+10) wat(i,j+10) wat(i+1,j+10) wat(i+2,j+10)];
                   wat(i,j)= mean(signal_matb);

      end
   end
end

%    Make an array with columns of zeros for missing minutes

wata=zeros(a(1),(length(var_step)+sum(var_step)));
stdwata=zeros(a(1),(length(var_step)+sum(var_step)));

i=1;
for j=1:(length(var_step))
   if var_step(j)==0
      wata(:,i)=wat(:,j);
      stdwata(:,i)=stdwat(:,j);
      alta(:,i)=Alt(:,j);
   else
      i=i+var_step(j)/step;
      wata(:,i)=wat(:,j);
      stdwata(:,i)=stdwat(:,j);
      alta(:,i)=Alt(:,j);
end
i=i+1;
```

```
end

wat=wata;
Alt=alta;
stdwat=stdwata;
clear stdwata wata alta;


Alt=Alt./1000;
a=size(Alt);



figure;

%   Check for columns of zeros.  If a column of zeros exists plot a white space
%   Check that the std of the measuremant is not > a * signal (a is a constant
%   inputted from the GUI screen.  If it is clip at the top.

for j=b:a(2)-b;
  for i=1:a(1)
          if (wat(:,j) == 0 | wat(:,j+1)==0 & (stdwat(:,j)==0 | stdwat(:,j+1)==0))
    break ; end;
     if ((stdwat(i,j) > sig_clip*wat(i,j)) | (stdwat(i,j+1) > sig_clip*wat(i,j+1) | i==a(1)));
       pcolor([j j+1],[Alt(1:(i-1),j) Alt(1:(i-1),j)],...
       [wat(1:(i-1),j) wat(1:(i-1),j+1)]);
      hold on;
       break; end;
      end
end

%   Plot labeling information

      if smooth == 1
      axis([10 (a(2)-10) Alt(1,1) Alt(a(1),1)])
      else
     axis([1 a(2) Alt(1,1) Alt(a(1),1)])
  end

shading interp;
h1=get(gca,'clim');
set(gca,'clim',[h1(1) maxval]);
barhan=colorbar('horiz');
axhan=gca;

h=title(name);
set(h,'fontname','timesnewroman','fontsize',14)
h=xlabel('Time (minutes)');
set(h,'fontname','timesnewroman','fontsize',12)
h=ylabel('Altitude (km)');
set(h,'fontname','timesnewroman','fontsize',12)
axes(barhan);
h=xlabel('Water Vapor Mixing Ratio (g/kg)');
set(h,'fontname','timesnewroman','fontsize',12)
axes(axhan);
```

```
%    Set the x axis label to the correct step size

if step ~=1
      h=get(gca,'xticklabel');
      set(gca,'xticklabel',num2str(step.*str2num(h)));
end

cd (save_loc);
setptr(1,'arrow');

%    For error in header

if (bitsetstart==1 & bitsetend==1)
  stringinput=('Both the beginning and ending minute - the integration time is < 0 ...  Please delete bad files
or enter title manually');
  bitsetstart=0; bitsetend=0;
  reply=warndlg(stringinput,'WARNING');
end

if (bitsetstart==1)
  stringinput=('The beginning minute - the integration time is < 0 ...  Please delete bad files or enter title
manually');
  reply=warndlg(stringinput,'WARNING');
end

if (bitsetend==1)
      stringinput=('The ending minute - the integration time is < 0...  Please delete bad files or enter title
manually');
  reply=warndlg(stringinput,'WARNING');
end
```